Electronic Supplementary Material (ESI) for Dalton Transactions.

Supplementary information

Protein sialylation affects the pH-dependent binding of ferric ion to human serum transferrin

Tomislav Friganović, Valentina Borko, and Tin Weitner*

Faculty of Pharmacy and Biochemistry, University of Zagreb, Ante Kovačića 1, 10000 Zagreb, Croatia

Corresponding author:
Tin Weitner, PhD
e-mail: tin.weitner@pharma.unizg.hr
tel.: +385 1 6394 452

Contents

1. Preparation and standardization of solutions

1.1. Preparation of working buffer solutions

The working buffer solutions were prepared by dissolving the appropriate amounts of solid substances in volumetric flasks. The flasks were filled with double-distilled water to about 80% of the total volume. The mixtures were briefly placed in an ultrasonic bath (a few minutes) to accelerate dissolution. The pH was then finely adjusted with aqueous HCl and/or NaOH. Water was added until the volume mark on the flask was almost reached, followed by a final pH adjustment. Further drops of water were then added to fill the flasks exactly to the marked line. The flasks were shaken vigorously after each addition of liquid and the pH electrode was always recalibrated before the working solutions were prepared. All working buffer solutions contained: 25 mM PIPES (piperazine-N,N′-bis(2-ethanesulfonic acid) dipotassium salt), 0.2 M KCl and 10 mM K_2CO_3. The pH values of the buffer solutions were adjusted to: 7.4, 6.9, 6.5, 6.2 and 5.9 during buffer preparation (in the volumetric flask).

1.2. Preparation and standardization of FeNTA solutions

The FeNTA stock solution was prepared by stepwise addition of ≈ 0.5 M Na_3NTA(aq) (pH ≈ 8.5) to a ≈ 0.5 M $FeCl_3$ solution (dissolved in 0.05 M HCl) in a molar ratio of 2 : 1. The Na_3NTA solution had previously been standardized by potentiometric titration with a NaOH standard solution to determine its exact concentration (c(Na_3NTA) = 0.4703 M). The pH of the resulting FeNTA stock solution was ≈ 2.2. ICP-MS analysis was performed to verify the exact iron concentration in the FeNTA stock solution.

The iron concentration in the FeNTA stock solution was determined using an Agilent 7900 ICP-MS instrument with an ASX-500 series autosampler and a quadrupole detector. In the first step, a calibration standard stock solution was prepared by diluting a commercially available Fe standard solution (9992 ± 30 µg/mL iron ICP standard in 5% HNO_3(aq), Inorganic Ventures, cat. no. CGFE10, lot no. P2-FE676240) by a factor of 100 in 1% v/v HNO_3. A calibration curve was then established by measurements on six different calibration standard solutions. These solutions were prepared by diluting the stock solution of the working calibration standard. An equal volume of an internal standard (1001 ± 4 µg/mL germanium ICP standard, tr. HNO_3 and HF) was added to each solution. The reference blank contained 1% HNO_3 and the internal standard. Six aliquots of the FeNTA sample were diluted 10,000-fold in 1% HNO_3. For this purpose, 10 µL of the sample was taken and diluted to 100 mL, adding 100 µL of the internal standard to each aliquot.

A nickel skimmer cone, a MicroMist nebulizer and a nickel sample cone were used for the measurements. Argon was used as the carrier gas at a flow rate of 1.2 L/min. Acquisition was performed in "He mode" using a collision cell with helium at 5 mL/min. General-purpose plasma mode and the pulse/analog detector mode were used. Data analysis was performed using MassHunter 4.1 ICP-MS Workstation software. The final iron concentration was calculated as the average of five replicate measurements, excluding one of the six aliquots due to experimental error in dilution. Subsequently, the FeNTA stock solution was divided into aliquots and stored at −20°C until further use. The final FeNTA solution contained: c(Fe) = 0.1505 M, c(NTA) = 0.3043 M with an estimated molar ratio of NTA : Fe = 1 : 2.022.

FeNTA working solutions were prepared by diluting the FeNTA stock solution in the titration buffer (25 mM PIPES, 10 mM K_2CO_3, 0.2 M KCl). pH corrections were performed as required. The FeNTA working solutions were always freshly prepared (immediately before performing the titration experiments). The dilution of the titration buffer by the FeNTA addition and the subsequent pH readjustments was less than 1 part per 1000. In our estimation, this source of error is small compared to

other sources of error in this study. The exact concentration of FeNTA in the working solutions was determined spectrophotometrically, as described in more detail in the following subsection.

1.3. Spectrophotometric determination of FeNTA concentration

The expression of the Beer-Lambert law for the FeNTA solutions (λ = 260 nm) can be written as shown in the Eq. S1:

$$\varepsilon_{\mathrm{NTA(260\ nm)}} c_{\mathrm{NTA}} + \varepsilon_{\mathrm{FeNTA(260\ nm)}} c_{\mathrm{FeNTA}} = \frac{A_{260\ \mathrm{nm}}}{l} \qquad \text{Eq. S1}$$

The spectral signal at λ = 260 nm is the result of the combined contributions of FeNTA and NTA species. NTA denotes species without iron (chelates of different protonation), while FeNTA denotes all chelated species containing iron. It is noteworthy that the molar absorption coefficient of the FeNTA species is about 3 orders of magnitude greater than that of the NTA species.[1] The same FeNTA stock solution was used for all experiments in this study. For this solution, the exact concentrations of both iron(III) and NTA species were determined as described in the previous subsection. Therefore, in all prepared FeNTA working solutions, the Fe : NTA ratio should match the 1 : 2.022 ratio used in the experiments to determine the molar absorption ratio.

The molar absorption coefficient for the FeNTA solution in the working buffer was calculated as $\varepsilon_{260\ \mathrm{nm}} = 5.93 \cdot 10^3\ \mathrm{M^{-1}\ cm^{-1}}$.[1] The molar absorption coefficient for the FeNTA stock solution was determined according to the following procedure. The FeNTA stock solution (c(Fe) = 0.1505 M and c(NTA) = 0.3043 M) was diluted 1000-fold in working buffer solution. To ensure precision and minimize possible pipetting errors due to the considerable volume ratios, each 1000-fold dilution was performed in three consecutive 10-fold dilutions. After each dilution step, vigorous shaking with a vortex mixer (Cole-Parmer, USA) was performed. Spectroscopic measurements were performed in a quartz glass cuvette with a light path length of 1 cm (Hellma, Germany). All spectrophotometric measurements were performed with a Varian Cary 50 Bio UV-Vis spectrophotometer (Varian, Australia). The averaged spectrum was calculated for all twelve replicates within each set. The baseline was determined by calculating the average of six replicate measurements. The final expression for FeNTA concentration is given[1] by Eq. S2:

$$c(\mathrm{FeNTA}) = \frac{\frac{A_{260\ \mathrm{nm}}}{l} - c_{\mathrm{NTA(total)}} \varepsilon_{\mathrm{NTA(260\ nm)}}}{\varepsilon_{\mathrm{FeNTA(260\ nm)}} - \varepsilon_{\mathrm{NTA(260\ nm)}}} \qquad \text{Eq. S2}$$

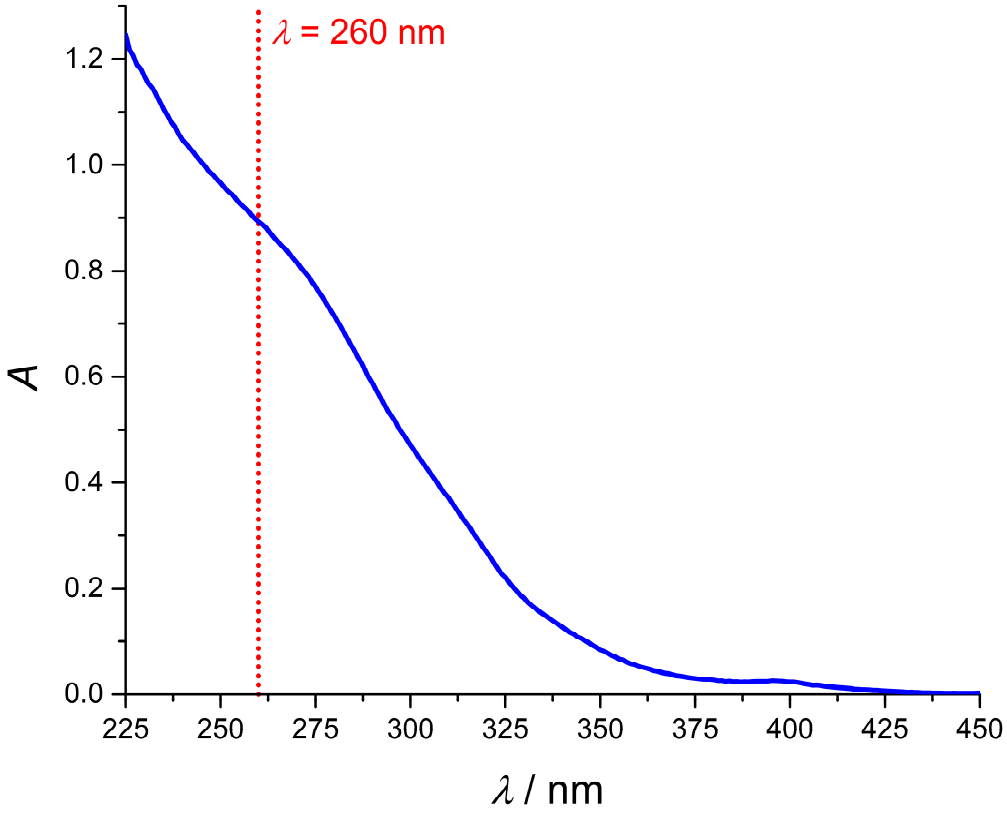

Figure S1. Example of the UV-Vis spectrum of the FeNTA working buffer solution (l = 1 cm, c(FeNTA) = 0.150 mM).

1.4. Preparation of hTf working solutions

The hTf working solutions were prepared by weighing and dissolving the appropriate amounts of hTf in the appropriate working buffers. The samples were briefly treated with the vortex mixer (Cole-Parmer, USA) to ensure proper dissolution. The pH was adjusted to the target values with small volumes of HCl(aq) and/or NaOH(aq). The exact protein concentrations were determined spectrophotometrically using the molar absorbance coefficients: ε_{280nm} = 84.4 x 10^3 M^{-1} cm^{-1} for Tf+S and ε_{280nm} = 84.8 x 10^3 M^{-1} cm^{-1} for Tf−S. The molar absorbance coefficient for Tf−S was determined in a previous study[2], while the coefficient for Tf+S was redetermined as described in the following subsection.

1.5. Redetermination of the molar absorbance coefficient for Tf+S

The molar absorbance coefficient for Tf+S was re-evaluated using the Edelhoch method, with measurements performed in decaplicate. The absorbance at λ = 280 nm of the folded protein was determined in a working buffer (25 mM PIPES, 0.2 M KCl, 10 mM K_2CO_3). Simultaneously, the absorbance at λ = 280 nm of the unfolded (denatured) protein was determined in the same buffer in the presence of 6 M guanidine-HCl. The molar absorbance coefficient ($\varepsilon_{folded,\ 280\ nm}$) for the folded protein was then calculated as the product of a reference molar absorbance coefficient for the unfolded protein ($\varepsilon_{unfolded,\ 280\ nm}$) and the ratio of the absorbance of the folded protein to that of the unfolded protein, as shown in Eq. S3:

$$\varepsilon_{\text{folded, 280 nm}} = \varepsilon_{\text{unfolded, 280 nm}} \cdot \frac{A_{\text{folded, 280 nm}}}{A_{\text{unfolded, 280 nm}}} \quad \text{Eq. S3}$$

The reference value for $\varepsilon_{\text{unfolded, 280 nm}}$ = 81080 M^{-1} cm^{-1} was calculated based on the contributions of 8 tryptophan, 26 tyrosine, and 19 cystine residues in the apo-transferrin structure.[2] These measurements were also performed in a quartz glass cuvette with a light path length of 1 cm (Hellma, Germany) using the Varian Cary 50 Bio UV-Vis spectrophotometer (Varian, Australia).

2. Enzymatic desialylation

2.1. Preparation of desialylated transferrin (Tf−S)

Desialylated apo-transferrin (Tf−S) was prepared according to the optimized protocol for SialEXO® (Genovis, Sweden).[3] Native transferrin (Tf+S) was first dissolved in a 20 mM TRIS buffer solution with a pH of 6.8. The pH was then adjusted to 6.8 with 1 M HCl and NaOH solutions. The mass concentration of transferrin was approximately 2.5 mg/mL. Specifically, 800 µL of the native transferrin solution was added to each of the four SialEXO® columns containing 2 sialidase enzymes derived from *Akkermansia muciniphila* and expressed in *E. coli*. This corresponds to approximately 8 mg of transferrin for each desialylation cycle. The SialEXO® columns were rotated on the tube revolver at 25 °C and 10 rpm for 48 hours. The protein was recovered by centrifugation (3 min, 1000 RCF). The SialEXO® columns have plastic caps on the bottom, which must be removed before the centrifugation step. After centrifugation, the enzyme beads remain in the SialEXO® columns while the protein solution is collected in 2 mL centrifuge tubes. This setup facilitates repeated desialylation cycles as fresh native transferrin can be added directly to the columns.

2.2. Preliminary FPLC assessment

To confirm sufficient desialylation, equal aliquots were taken from all 2 mL centrifuge tubes (each containing approximately 2 mg asialotransferrin) and pooled. The pooled protein contained 200 µL (≈ 0.5 mg), which we considered to be sufficient for chromatographic analysis. The chromatographic experiment was performed on the ÄKTApurifier 10 FPLC instrument (Cytiva, USA) using the isoelectric focusing method, as the pI values of native and asialotransferrin differ significantly.[2]

pISep pH gradient buffers (CryoBioPhysica, USA, cat. No. 20055) were prepared by mixing the appropriate amounts of pISep starting buffers. Elution buffer 1 with a pH of 7.4 consisted of 50.3% pISep A and 49.7% pISep B. Elution buffer 2 with a pH of 5.5 consisted of 67.56% A and 32.44% B. 600 µL of elution buffer 1 was added to 200 µL of the pooled protein sample. For each sample, the pH was adjusted to 7.4 or a very close value above (up to pH = 7.5) by adding HCl(aq) and/or NaOH(aq). The Source 15Q 4.6/100 PE anion exchange column was used for the experiments. Chromatofocusing was performed with a one-step linear gradient phase supplemented by two short isocratic intervals, starting with 100% buffer 1 and ending with 100% buffer 2. The flow rate was maintained at 0.5 mL/min throughout the experiment, with absorbance measurements recorded at λ = 280 nm and l = 1 cm. Similarly, we subjected native apo-transferrin (Tf+S) to chromatofocusing for comparison. The resulting chromatograms (Figure S2) for Tf+S and Tf−S were in good agreement with previously published results, indicating successful desialylation.[2]

All asialotransferrin samples prepared in the 17 consecutive desialylation cycles were pooled and concentrated by centrifugal filtration using Amicon® Ultra centrifugal filters (0.5 mL, MWCO 30 K, Merck Millipore, USA, cat. no. UFC503096). Each centrifugation step was performed for 5 minutes and at 14000 RCF. The concentrates were thoroughly washed five times with pure water and then centrifuged as described above. These concentrates were then transferred to several 200 µL tubes and stored at −20 °C until further use.

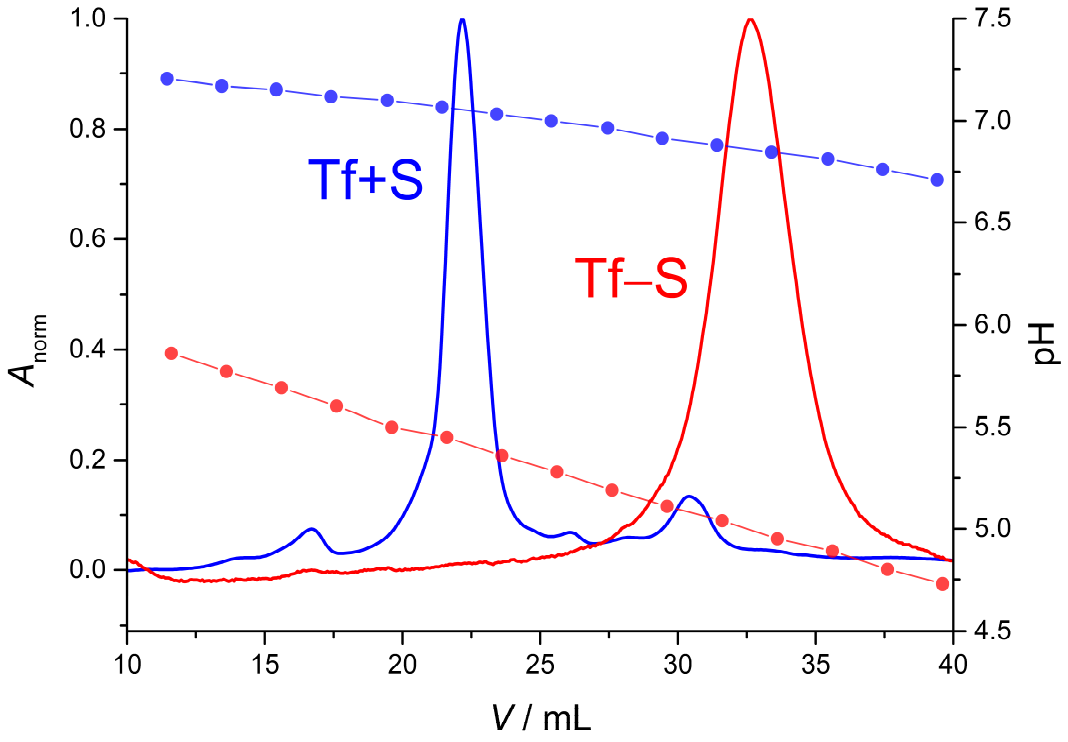

Figure S2. FPLC pH gradient ion-exchange chromatograms of native human apo-transferrin (Tf+S, blue) and desialylated human apo-transferrin (Tf−S, red). For the sake of clarity, the absorbance values for each experiment are normalized as $A_{i,\,norm} = A_{i,\,norm} / A_{max}$. The solid curves depict normalized absorbance values (λ = 280 nm chromatographic signals), while the connected dots on the line represent the measured pH values.

2.3. UHPLC N-glycan analysis

UHPLC analysis of N-glycans was performed according to the procedure described in a previous study.[2] The analysis was performed for both native (Tf+S) and desialylated (Tf−S) human apo-transferrin. Briefly, the required amount of protein concentrate corresponding to 200 µg of native (Tf+S) or desialylated (Tf−S) apo-transferrin was dissolved in 50 µL of freshly distilled water. The samples were then dried in a vacuum centrifuge. The samples were denatured by adding 30 µL of a 1.33% (w/v) SDS solution and incubated at 65 °C for 10 minutes. After denaturation, 10 µL of a 4% (v/v) Igepal-CA630 solution was added to the samples and the mixture was shaken on a plate shaker for 15 minutes. The N-glycans were then released by adding 1.2 U PNGase F and incubated overnight at 37 °C.

The free N-glycans were labeled using the following labeling mixture:

(i) 2-aminobenzamide (2-AB) (19.2 mg/mL; Sigma Aldrich, USA)
(ii) 2-picoline borane (44.8 mg/mL; Sigma Aldrich, USA)
(iii) mixture of dimethyl sulfoxide (Sigma Aldrich, USA) and glacial acetic acid (Merck, Germany) mixture (70:30 v/v).

To each sample, 25 µL of the labeling mixture was added and the samples were then incubated at 65 °C for 2 hours. Free markers and reducing agents were then removed from the samples by hydrophilic

interaction liquid chromatography solid-phase extraction (HILIC-SPE). After the incubation period, 700 µL of acetonitrile (ACN) was added to the samples to achieve a final concentration of 96% ACN by volume. The samples were then applied to individual wells of a 0.2 µm GHP filter plate. The solvent was removed by vacuum application using a vacuum manifold. All wells were first pre-washed with 70% ethanol and water, followed by equilibration with 96 % ACN. The loaded samples were then washed 5 times with 96% ACN. Finally, the N-glycans were eluted with water and stored at −20 °C until further use.

Fluorescently labeled N-glycans were separated by hydrophilic interaction chromatography using an Acquity UPLC H-Class instrument (Waters, USA). This instrument contains a quaternary solvent manager, a sample manager, and a fluorescence detector with an excitation wavelength of λ_{ex} = 250 nm and an emission wavelength of λ_{em} = 428 nm. The device was controlled by Empower 3 software (build 3471, Waters, USA). The labeled N-glycans were separated on a Waters BEH glycan chromatography column, where solvent A was 100 mM ammonium formate at pH = 4.4 and solvent B was ACN. The separation method involved a linear gradient from 70% to 53% acetonitrile with a flow rate of 0.56 mL/min during a 25-minute analytical run. The system was calibrated with an external standard of hydrolyzed and 2-AB-labeled glucose oligomers, which allowed the conversion of retention times for individual glycans to glucose units (GU).

The recorded chromatograms were preprocessed by replacing negative values in the chromatographic signals with 0. This was achieved using the IF() function in Microsoft Excel. Subsequently, the chromatographic peaks corresponding to the signals of the labeled glycans were identified and integrated within the retention time window of 4 to 20 minutes. The very intense peak with a maximum at about 0.7 minutes, corresponding to the free fluorescent labeling molecule, was excluded from the analysis. Based on data from a previous UHPLC-MS analysis, the N-glycan peaks were determined by comparing their retention times and peak shapes with those previously observed. Integration of the signals was performed using the custom Python script. Specifically, the function np.trapz() from the NumPy library was used, which employs the composite trapezoidal rule for integration. The percentages of glycans were determined by multiplying the integrals corresponding to the chromatographic peaks of the specific glycans by 100 and dividing by the difference of the total integral minus the integral of the residual noise.

The extent of transferrin desialylation was estimated using the values of the index of sialylation (*IS*) according to Eq. S4.

$$IS = \sum_{i=1}^{n} f_i \cdot s_i \qquad \text{Eq. S4}$$

n represents the N-glycan fraction number, f_i denotes the percentage content of the specific N-glycan fraction, and s_i indicates the number of sialic acids within the structure of the corresponding N-glycan fraction. The obtained *IS* values for Tf+S = 127.79 and Tf−S = 1.51 confirmed a remarkable ≈ 99% reduction in sialic acid content for the enzymatically desialylated protein (Tf−S). The UHPLC chromatograms (and the corresponding glycan structures) are shown in Figure S3.

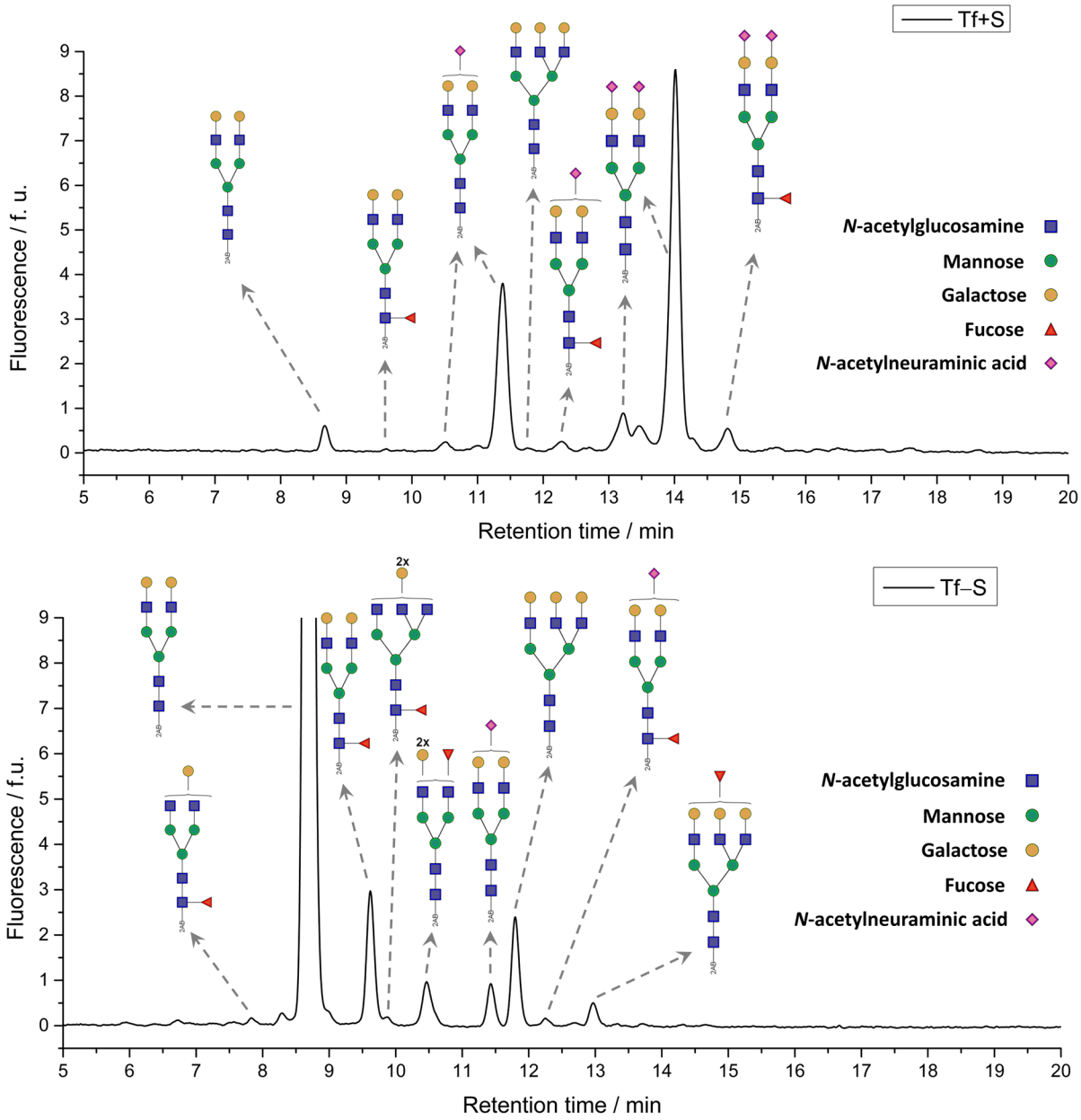

Figure S3. UHPLC chromatograms showing the assigned N-glycan residues in native apo-transferrin (Tf+S, **top**) and desialylated apo-transferrin (Tf−S, **bottom**).

3. Titration methods

3.1. Titrating liquids into microcentrifuge tubes

All liquid samples in the titration experiments were prepared using the Opentrons OT-2 pipetting robot (Opentrons, USA). The first generation (GEN1) P-20 and P-300 pipettes were used together with the corresponding original Opentrons pipette tips. The protocols for these specific experiments were created using custom Python scripts and tab-delimited tables containing the specified volumes for pipetting. Solutions were pipetted from the 5 mL or 50 mL plastic tubes into the 500 µL microcentrifuge tubes. All plastic tubes were secured in their respective customized 3D-printed holders. Pipetting was performed by gradually lowering the relative height of the pipette tip, considering the previously transferred liquid volume (the optimal height was determined for each step based on the geometric parameters of the labware depending on the transferred volume). This was done to ensure uniform immersion of the tip(s) and to avoid possible errors due to unequal hydrostatic pressures and possible deposition of the liquid on the outer layer of the tip (dripping could be observed if the tip is immersed too deeply into the solution).

Each titration experiment consisted of two separate steps: in the first step (i), only the non-protein components were mixed; in the second step (ii), the protein solution was added to the mixture. The addition of the non-protein components (i) was performed by first pipetting all volumes > 30 µL with a single pipette tip per compound. This was done from a relatively high tip position within the 500 µL microtube to avoid possible contamination of the tip by contact with other liquids. Volumes ≤ 30 µL were then added directly to the liquid present (2 mm from the bottom of the 500 µL microtube). After the addition of each volume ≤ 30 µL, the pipette tip was rinsed in place and a blow-out procedure was performed to ensure complete transfer of the liquid.

The protein component (ii) was added to the non-protein mixture (2 mm from the bottom of the 500 µL microtube) and rinsed with blowout. The protein solutions were added directly to the non-protein mixture due to viscosity and adhesion problems (bubble formation and incomplete volume transfer were observed when the protein was added without tip immersion). To avoid cross-contamination, pipette tips were replaced after each volume addition that required tip immersion in the 500 µL microtube. The total volumes in the titrations were either 300 or 500 µL per microtube. The protein-containing substance accounted for only 1/3 or at most 1/2 of the total volume. After completion of the titration, each 500 µL microtube was capped and mixed with the vortex mixer. The samples were then equilibrated for >1 day at 25° C.

3.2. Transferring samples to 96-well microplates

After the equilibration phase, the microtubes were mixed on a vortex mixer, decapped, and placed in a suitable holder in the OT-2 pipetting robot. 200 µL of each sample from the 500 µL microtube was pipetted into the 96-well plate. The pipette tip was changed for each sample to prevent possible cross-contamination. Samples were added to the microtiter plate at (pseudo-)randomized positions. Randomization was performed via a custom Python script and was done to reduce possible systematic errors due to possible irregularities in the microtiter plate, anisotropy of positions (e.g. wells in the middle and at the edge of the microtiter plate) and/or other effects that could strongly apply to the adjacent positions in the microtiter plate.

4. Fluorescence and absorbance

4.1. Fluorescence measurements

Fluorescence was measured with the Tecan Spark M10 (Tecan, Austria) multimode microplate reader using the 96-well UV-Vis transparent microplates (black, μ-clear, flat bottom, chimney well, Greiner, USA, cat. no. 655097). For each set of measurements, the *z*-position (the vertical distance between the optical element and the bottom of the microplate well) was first optimized using the optimization method built into the reader's software.[4] The optimal *z*-position is the height of the optical element which produces the strongest fluorescence response. Optimization of the *z*-position was always performed for the apo-transferrin sample, as this is the sample that produces the strongest fluorescence response within a given titration set (as iron binding to transferrin quenches protein fluorescence). This optimization was performed separately for each titration experiment. The optimal values determined are all very similar and are around 17000 μm, with less than 1 % deviation. In addition to the optimal *z*-positions, several additional fixed *z*-positions were used for data acquisition in all titrations (as indicated in Table S1), mainly for the purpose of subsequent IFE (Inner Filter Effect) correction.

The gain parameter was also optimized separately for each set before the fluorescence measurements. The gain represents the amplification factor applied to the photomultiplier tube (PMT) detector and influences the measurement sensitivity. In general, measuring at higher gain values should improve the sensitivity of fluorescence measurements. On the other hand, over-amplification can saturate the signal and thus overload the detector. For this reason, the gain for the apo-transferrin samples (which give the strongest fluorescence response within a given titration) was optimized using the optimized *z*-position value (as this height of an optical element produces the maximum fluorescence response within a given range of *z*-positions). All measurements at the different *z*-positions for a given titration experiment were always recorded with the same gain value.

The fluorescence measurements were performed with an excitation wavelength λ_{ex} = 280 nm and an emission wavelength λ_{em} = 335 nm. These measurements were performed in top-reading mode, where both the light source and the detector were positioned above the microplate well. Excitation at 280 nm is commonly used for various fluorescent proteins. The emission wavelength of 335 nm was chosen because it produces a strong fluorescence signal near the emission maximum while minimizing the crosstalk effect. Crosstalk is the overlap of the fluorescence excitation radiation and the emitted signal. For the specific microplate reader that we used in our experiments, it is recommended to measure at a spectral difference $\lambda_{em} - \lambda_{ex} \geq 45$ nm. In our measurements, this difference was 55 nm. We also used a suitable optical filter for excitation (280 nm, bandwidth 15 nm, Tecan, Austria, cat. no. 30092080) mounted on a custom-made 3D-printed holder to ensure that the excitation light did not contribute to the fluorescence signal. An empty microplate was examined for possible overlap, as shown in Figure S4.

Table S1. The *z*-position values used for the fluorescence measurements.

z-position / µm
optimized ≈ 17000
14600
15000
15500
16000
17000
18000
19000
20000
21000

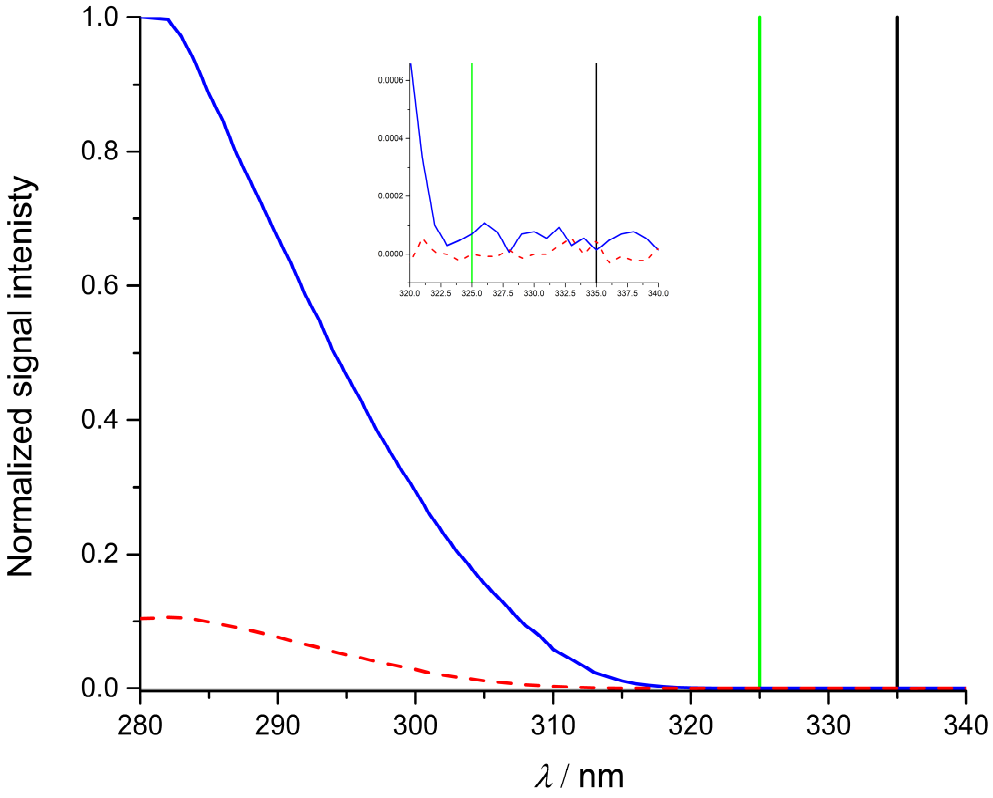

Figure S4. Results of fluorescence measurements (λ_{ex} = 280 nm) of an empty 96-well microplate with (red dashed line) and without (solid blue line) use of an optical filter. The spectra were normalized by setting the point with the highest fluorescence signal as reference. The green vertical line represents the crosstalk threshold $\lambda_{em} - \lambda_{ex} \geq 45$ nm (λ_{em} = 325 nm) recommended by the manufacturer of the microplate reader (Tecan, Austria). The black vertical line represents the value of λ_{em} = 335 nm used in this work. **Inset:** An enlarged section of this plot in the range of λ_{em} 320-340 nm.

4.2. Absorbance measurements

The absorbance values of the protein and FeNTA solutions used for the titrations were measured with the Varian Cary 50 Bio UV-Vis spectrophotometer (Varian, Australia) using a quartz glass cuvette with a path length of l = 1 cm (Hellma, Germany). The absorbances of the titration samples were measured in the range of 200-1000 nm in 1 nm steps in the 96-well microplates (black, μ-clear, flat bottom, chimney well, Greiner, USA, cat. no. 655097) on the Tecan Spark M10 (Tecan, Austria) multimode microplate reader.

5. Fluorescence data

5.1. Inner Filter Effect (IFE) corrections

IFE corrections were performed using the ZINFE (Z-position INner Filter Effect) method, as previously described.[4] ZINFE method utilizes the differences in the measured fluorescence at variable heights (*z*-positions) of light source/detector. The method can be described by Eq. S5.

$$F_Z = F_{0(z_1)} \left(\frac{F_{0(z_2)}}{F_{0(z_1)}}\right)^{\frac{k-z_2}{z_2-z_1}} \quad \text{Eq. S5}$$

F_Z represents the fluorescence intensity corrected with ZINFE. $F_{0(z1)}$ and $F_{0(z2)}$ denote measured fluorescence values at different *z*-positions, z_1 and z_2, while k is a geometric parameter that only applies to a specific combination of sample volume, microplate, and microplate reader. For the volume of 200 µL per microplate well, the geometric parameter k was estimated to be 20593 µm.[4] The ZINFE corrections were performed with $F_{0(z1)}$ measured at the optimized value of $z \approx 17000$ µm, while $F_{0(z2)}$ was measured at $z = 20000$ µm.

This technique was developed specifically for microplate readers and has been shown to be effective for absorbance values up to approximately $A_{ex} \approx 2$, $A_{em} \approx 0.5$.[4] The absorbance values obtained in hereby presented experiments are well below these thresholds, suggesting suitability of ZINFE correction procedure for this study. To further confirm our claim that the ZINFE method is suitable, the measured fluorescence was also processed using the common IFE correction method proposed by Lakowicz in his popular textbook on fluorescence spectroscopy.[5] As mentioned in the literature, the Lakowicz correction loses its effectiveness at absorbance values > 0.7.[4,6,7] This limit is more than twice as high as the absorbance that occurs in the experiments presented here. The Lakowicz correction procedure is shown in Eq. S6.

$$F_A = F_0 \cdot 10^{\left(\frac{A_{ex}+A_{em}}{2}\right)} \quad \text{Eq. S6}$$

F_A is the IFE-corrected fluorescence, F_0 is the uncorrected (measured) fluorescence, A_{ex} and A_{em} are the absorbance at the excitation and emission wavelengths, respectively. As expected, the two methods described above yielded very similar results. This becomes particularly clear when the results of one method are plotted against the results of the other, as shown in Figs. S5 and S6. The coefficients of determination obtained by regressing the results of one correction against the other are $R^2 > 0.99$ in all cases, as can be seen in Table S2.

Table S2. R^2 values obtained from the linear regressions using two different IFE correction methods.

	pH	5.9	6.2	6.5	6.8	7.4
R^2	Tf+S	0.9932	0.9946	0.9990	0.9986	0.9991
	Tf–S	0.9995	0.9981	0.9997	0.9982	0.9996

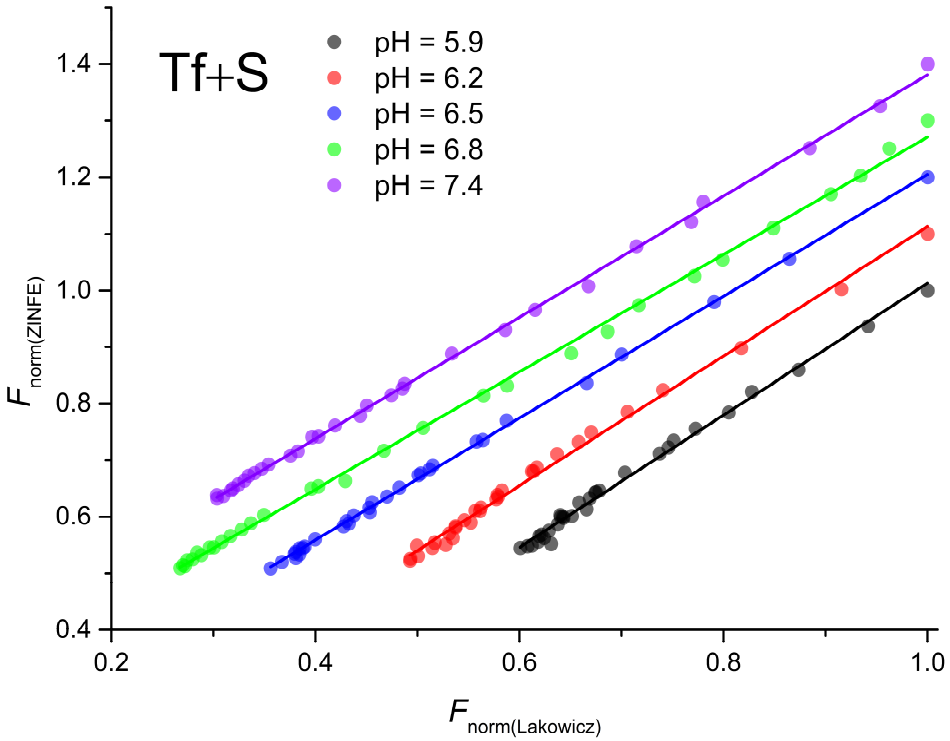

Figure S5. ZINFE IFE correction as a function of Lakowicz IFE correction for Tf+S (native human apo-transferrin) titrations. The values are normalized as $F_{i,\mathrm{norm}} = F_i / F_{\mathrm{max}}$. For visual clarification, the linear interpolations ($y = a + bx$) are shifted by value $a_{\mathrm{shifted}} = a + n \cdot 0.1$ for each increasing pH value, $n = 0, 1, 2, 3, 4$; for pH = 5.9, 6.2, 6.5, 6.8, 7.4, respectively.

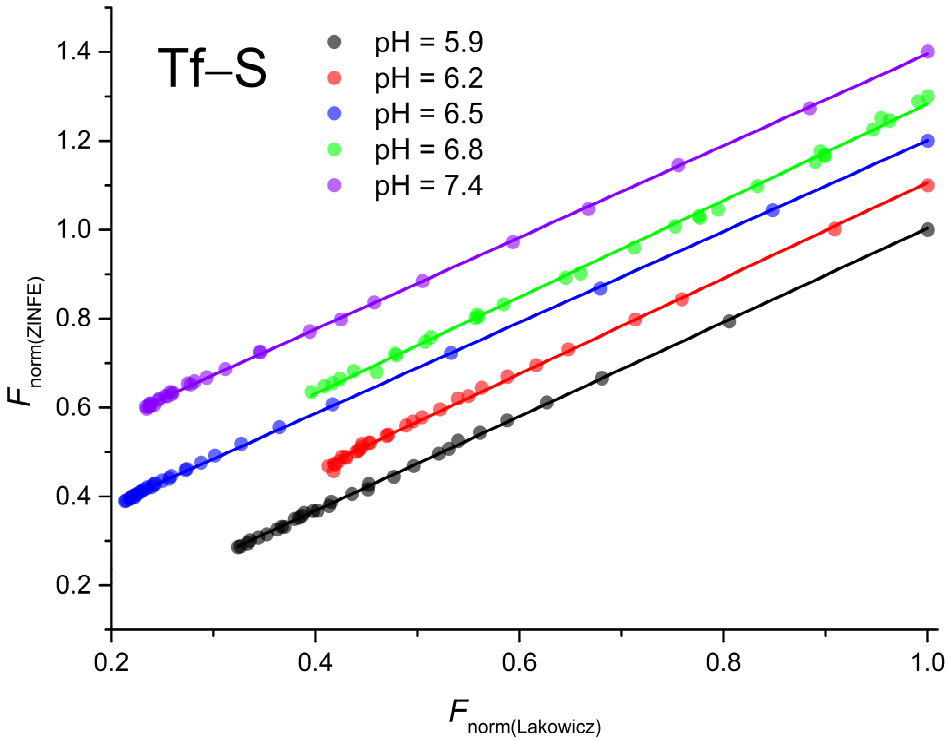

Figure S6. ZINFE IFE correction as a function of Lakowicz IFE correction for Tf–S (desialylated human apo-transferrin) titrations. The values are normalized as $F_{i,\mathrm{norm}} = F_i / F_{\mathrm{max}}$. For visual clarification, the linear interpolations ($y = a + bx$) are shifted by value $a_{\mathrm{shifted}} = a + n \cdot 0.1$ for each increasing pH value, n = 0, 1, 2, 3, 4; for pH = 5.9, 6.2, 6.5, 6.8, 7.4, respectively.

5.2. Fluorometric titrations for determination of the active protein fraction

The values of the relative fluorescence of Fe_2Tf (s = 0.174 for Tf+S and s = 0.183 for Tf−S) were determined in the 'titration regime' defined by Jarmoskaite *et al*. in their considerations on 1:1 binding experiments.[8] Under these conditions, the concentration of the constant component is much higher than the K_D, so that essentially all of the added titrant is depleted from the solution by binding to the titrand until there is no more free titrand to bind. In this case, the concentration of titrant that results in half binding is not equal to the K_D. However, these conditions are suitable for determining the titrand content and the fluorescence signal corresponding to complete saturation of the binding sites.

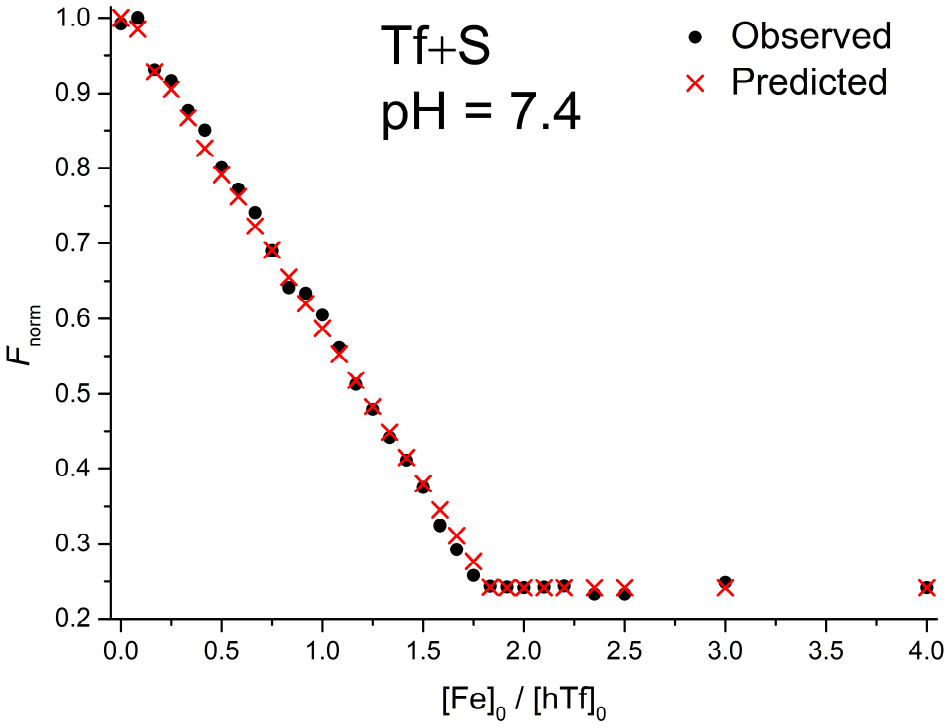

Figure S7. Measured (F_{obs}) and calculated (F_{calc}) normalized fluorescence for fluorometric titration of human serum transferrin (Tf+S) with FeNTA: $[hTf]_0$ = 1.93 µM, [PIPES] = 25 mM, [KCl] = 0.2 M, $[HCO_3^-]$ = 10 mM, $[NTA]_0$ = 0 mM, pH = 7.4, 25 °C.

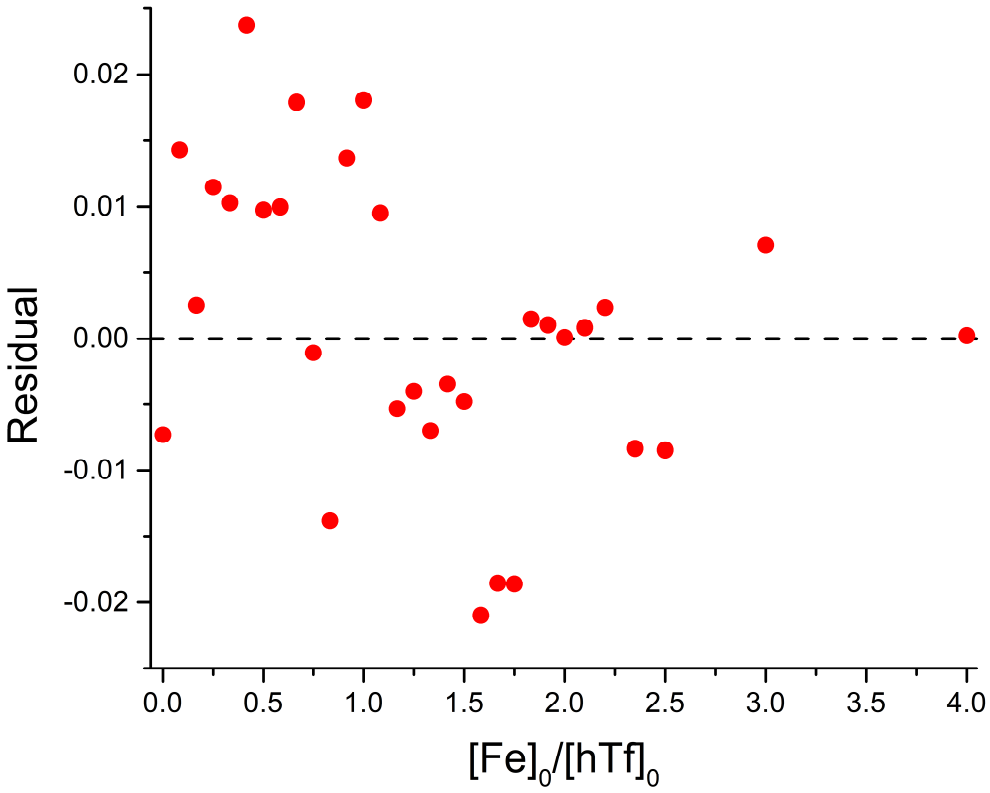

Figure S8. Residuals of the fit related to the experiment shown in Figure S7, calculated as $F_{calc} - F_{obs}$.

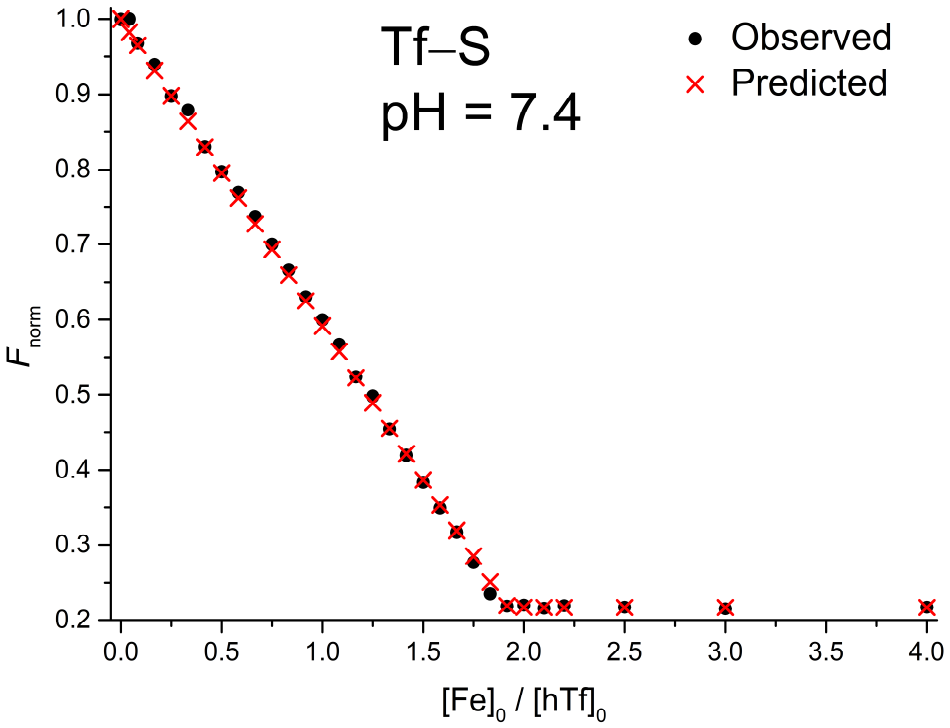

Figure S9. Measured (F_{obs}) and calculated (F_{calc}) normalized fluorescence for fluorometric titration of desialylated human serum transferrin (Tf–S) with FeNTA: $[hTf]_0$ = 2.09 μM, [PIPES] = 25 mM, [KCl] = 0.2 M, $[HCO_3^-]$ = 10 mM, $[NTA]_0$ = 0 mM, pH = 7.4, 25 °C.

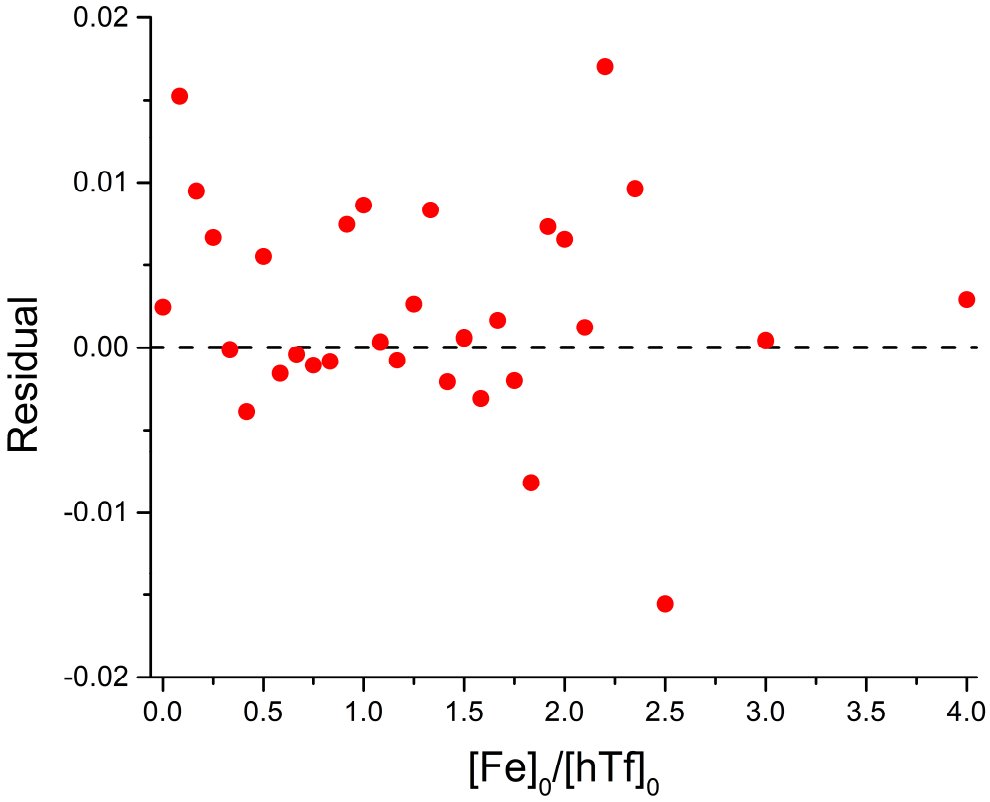

Figure S10. Residuals of the fit related to the experiment shown in Figure S9, calculated as $F_{calc} - F_{obs}$.

5.3. Fluorometric titrations for determination of the apparent binding constants

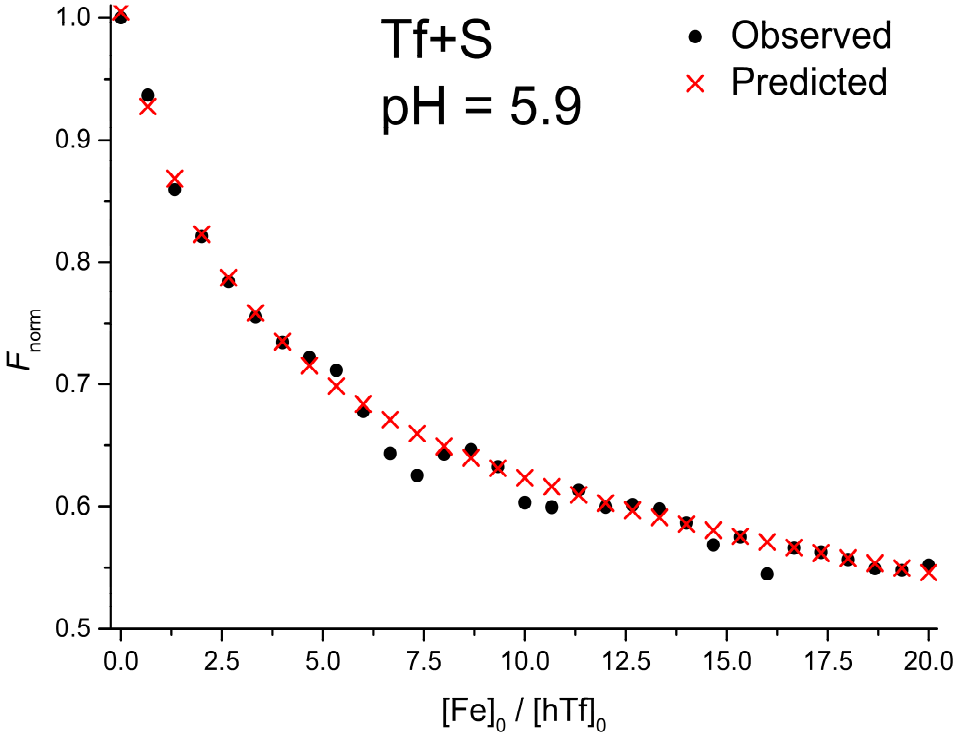

Figure S11. Measured (F_{obs}) and calculated (F_{calc}) normalized fluorescence for the spectrofluorometric titration of human serum transferrin (Tf+S) with FeNTA: $[hTf]_0$ = 1.78 µM, [PIPES] = 25 mM, [KCl] = 0.2 M, $[HCO_3^-]$ = 10 mM, $[NTA]_0$ = 0.1 mM, pH = 5.9, 25 °C. The parameters determined with the Solver tool in Microsoft Excel for the calculation of F_{calc} are: $\log(K_{1m})$ = 5.425 ± 0.012, $\log(R)$ = 1.541, ± 0.008 R^2 = 0.9913.

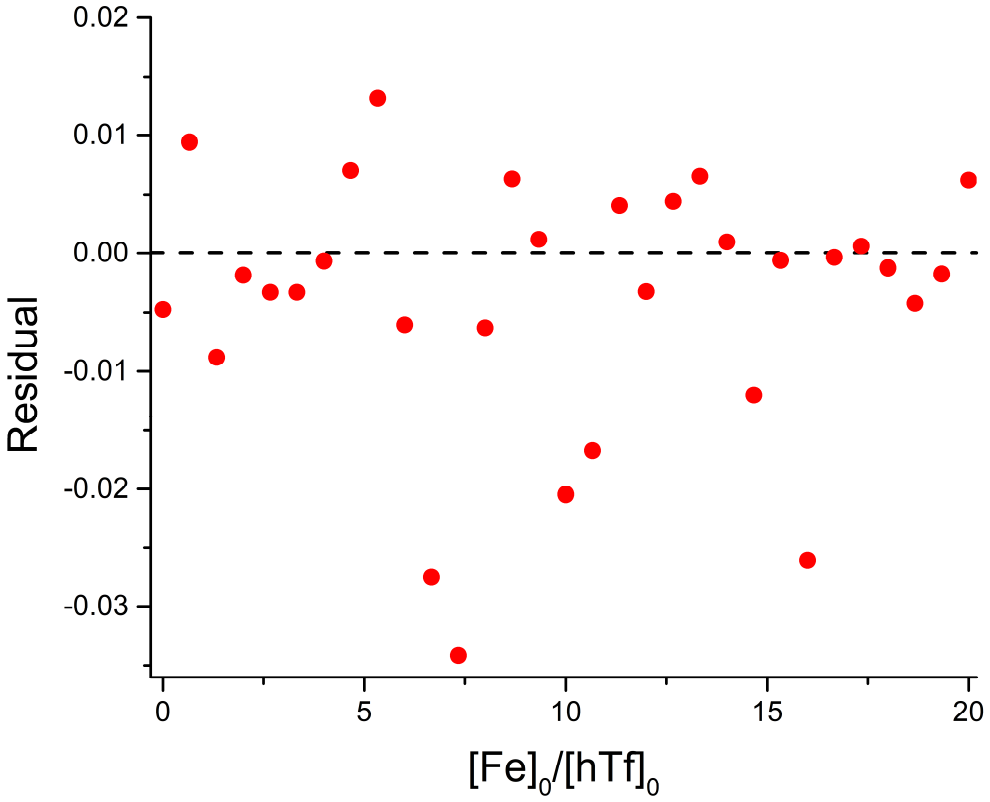

Figure S12. Residuals of fit related to experiment presented in Figure S11 calculated as $F_{calc} - F_{obs}$.

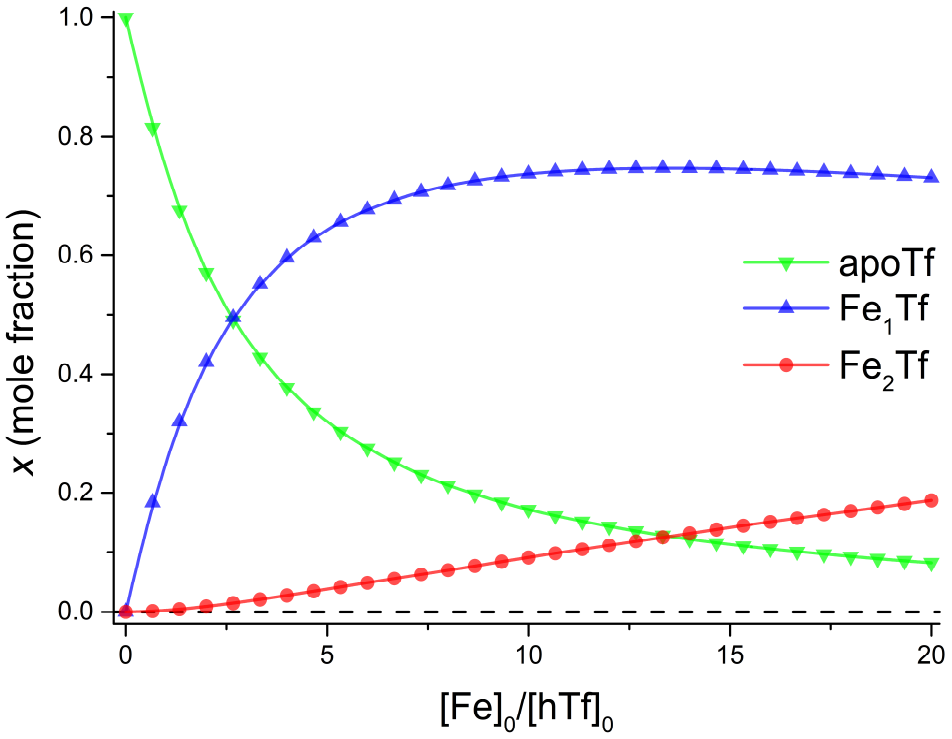

Figure S13. Transferrin speciation related to experiment presented in Figure S11 according to Eqs. 9-11 in the manuscript.

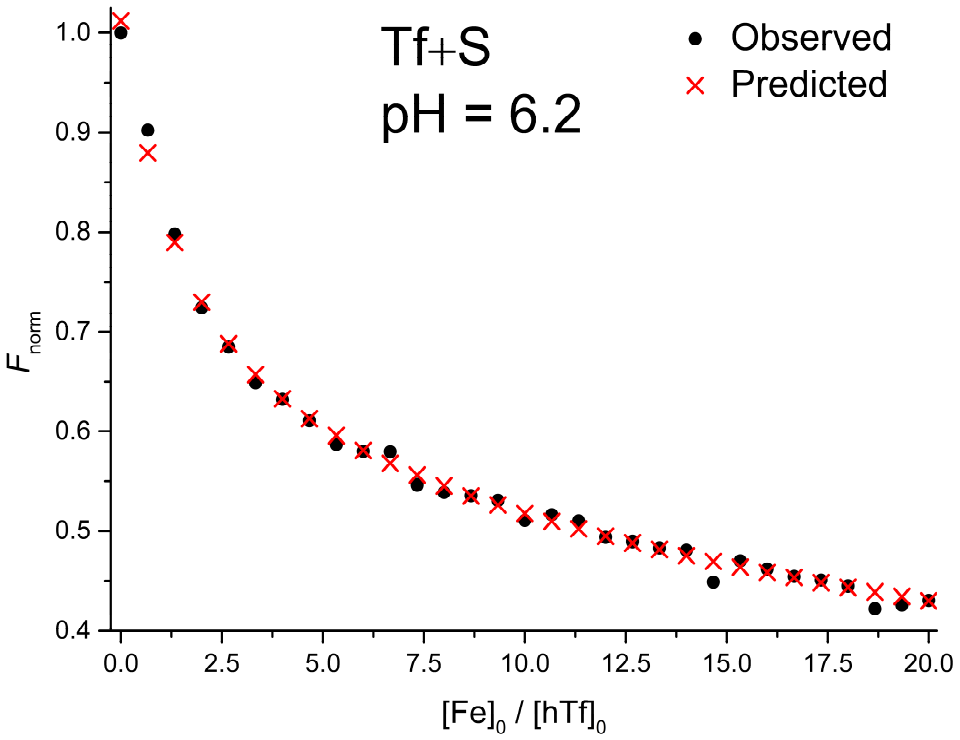

Figure S14. Measured (F_{obs}) and calculated (F_{calc}) normalized fluorescence for the spectrofluorometric titration of human serum transferrin (Tf+S) with FeNTA: $[hTf]_0$ = 2.05 µM, [PIPES] = 25 mM, [KCl] = 0.2 M, $[HCO_3^-]$ = 10 mM, $[NTA]_0$ = 0.5 mM, pH = 6.2, 25 °C. The parameters determined with the Solver tool in Microsoft Excel for the calculation of F_{calc} are: $\log(K_{1m})$ = 5.812 ± 0.065, $\log(R)$ = 1.522 ± 0.041, R^2 = 0.9960.

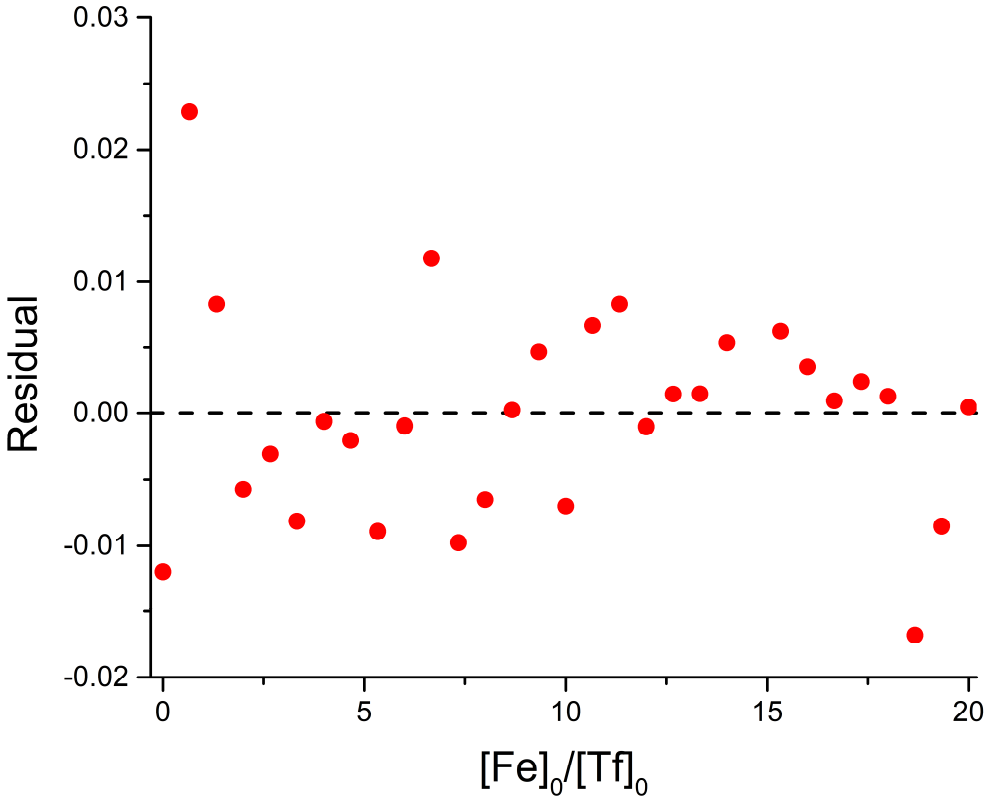

Figure S15. Residuals of fit related to experiment presented in Figure S14 calculated as $F_{calc} - F_{obs}$.

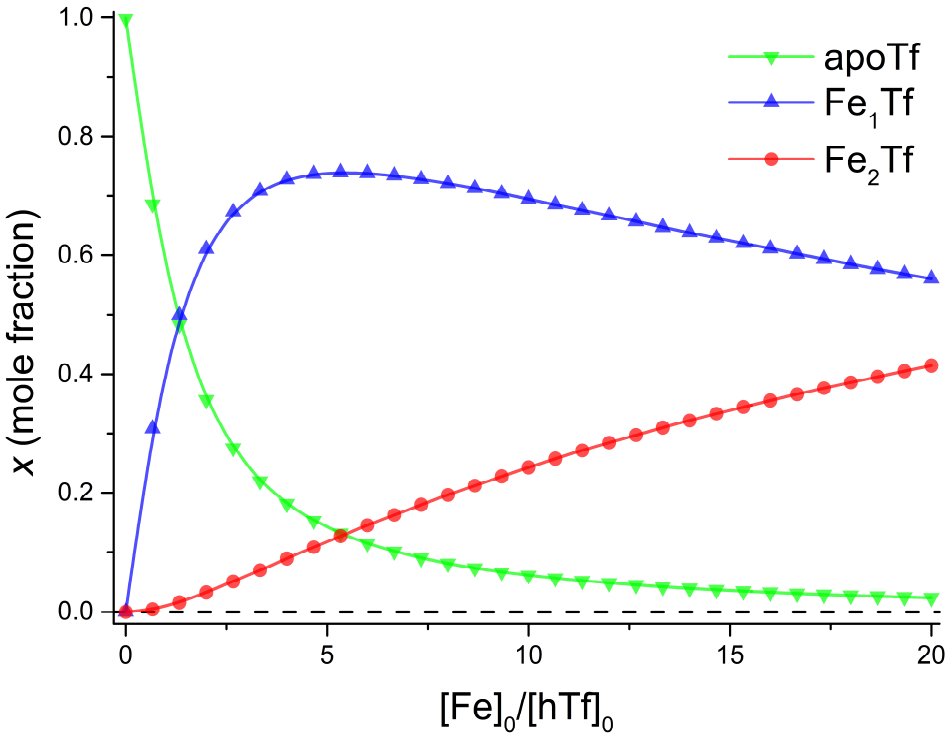

Figure S16. Transferrin speciation related to experiment presented in Figure S14 according to Eqs. 9-11 in the manuscript.

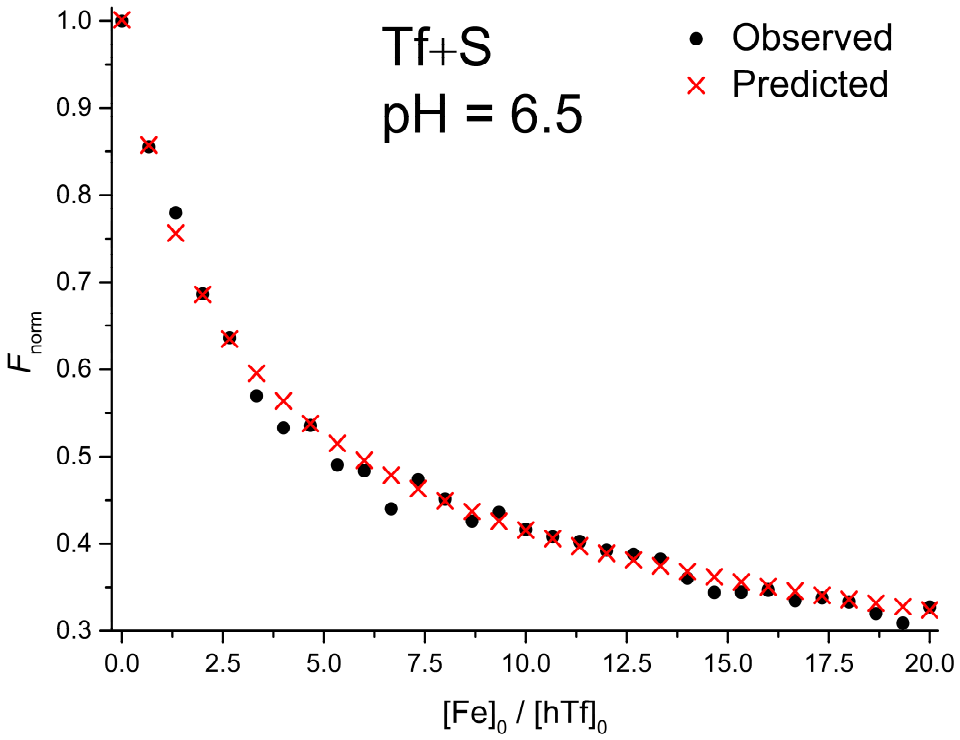

Figure S17. Measured (F_{obs}) and calculated (F_{calc}) normalized fluorescence for the spectrofluorometric titration of human serum transferrin (Tf+S) with FeNTA: $[hTf]_0$ = 2.04 µM, [PIPES] = 25 mM, [KCl] = 0.2 M, $[HCO_3^-]$ = 10 mM, $[NTA]_0$ = 0.5 mM, pH = 6.5, 25 °C. The parameters determined with the Solver tool in Microsoft Excel for the calculation of F_{calc} are: $\log(K_{1m})$ = 5.887 ± 0.032, $\log(R)$ = 1.176 ± 0.022, R^2 = 0.9938.

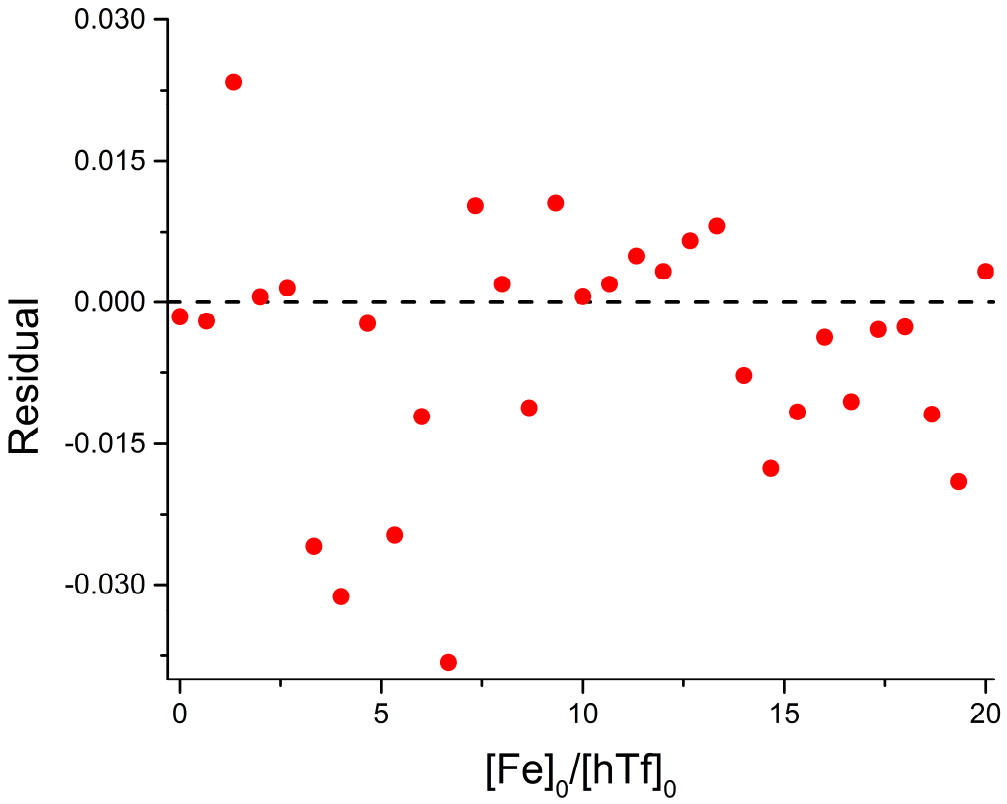

Figure S18. Residuals of fit related to experiment presented in Figure S17 calculated as $F_{calc} - F_{obs}$.

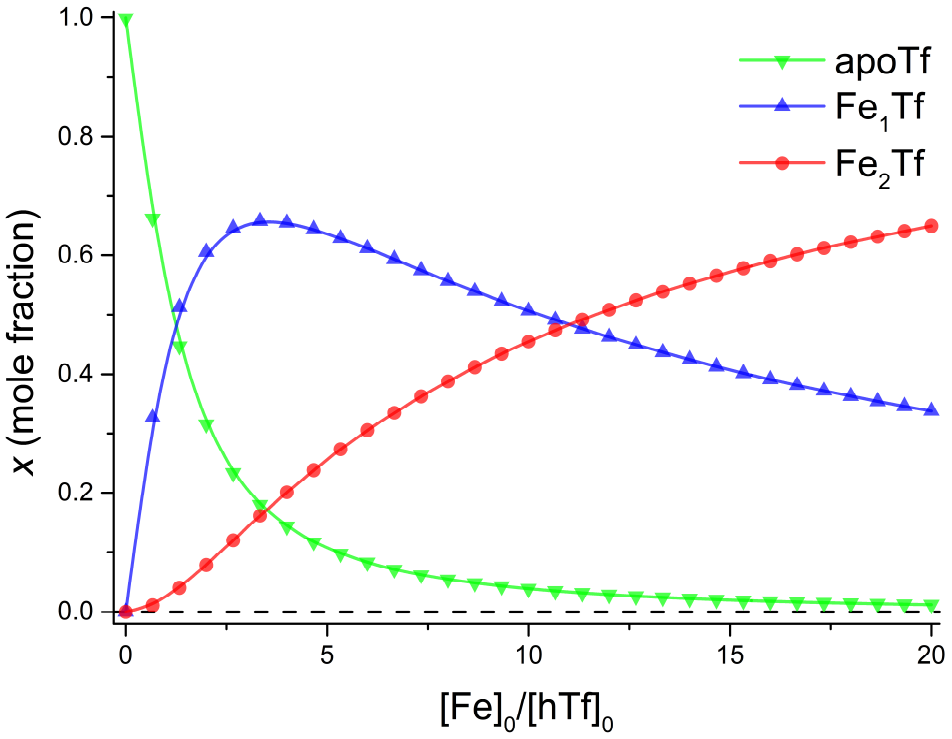

Figure S19. Transferrin speciation related to experiment presented in Figure S17 according to Eqs. 9-11 in the manuscript.

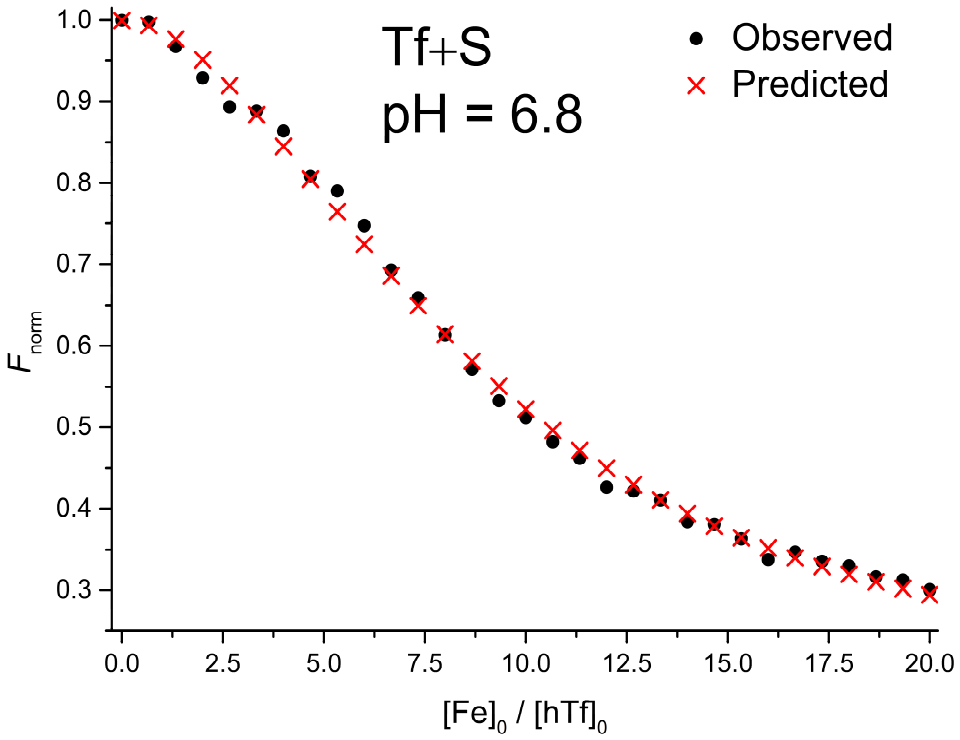

Figure S20. Measured (F_{obs}) and calculated (F_{calc}) normalized fluorescence for the spectrofluorometric titration of human serum transferrin (Tf+S) with FeNTA: $[hTf]_0$ = 2.27 μM, [PIPES] = 25 mM, [KCl] = 0.2 M, $[HCO_3^-]$ = 10 mM, $[NTA]_0$ = 10 mM, pH = 6.8, 25 °C. The parameters determined with the Solver tool in Microsoft Excel for the calculation of F_{calc} are: $\log(K_{1m}) = 0 \pm 0$, $\log(R) = -9.532 \pm 0.014$, $R^2 = 0.9971$. At pH = 6.8, the calculated $\log(K_{1m})$ and $\log(R)$ are not meaningful because the second iron ion binding event may dominate and possibly mask the effects of the first binding event, leading to incorrect values of the equilibrium constant.

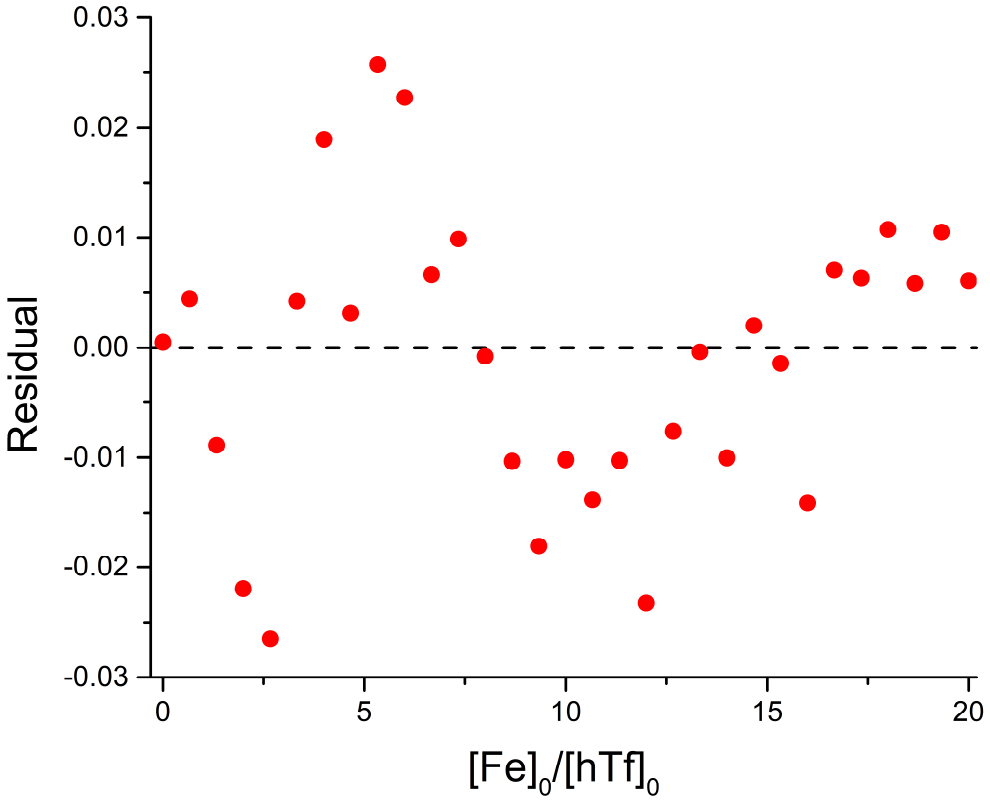

Figure S21. Residuals of fit related to experiment presented in Figure S20 calculated as $F_{calc} - F_{obs}$.

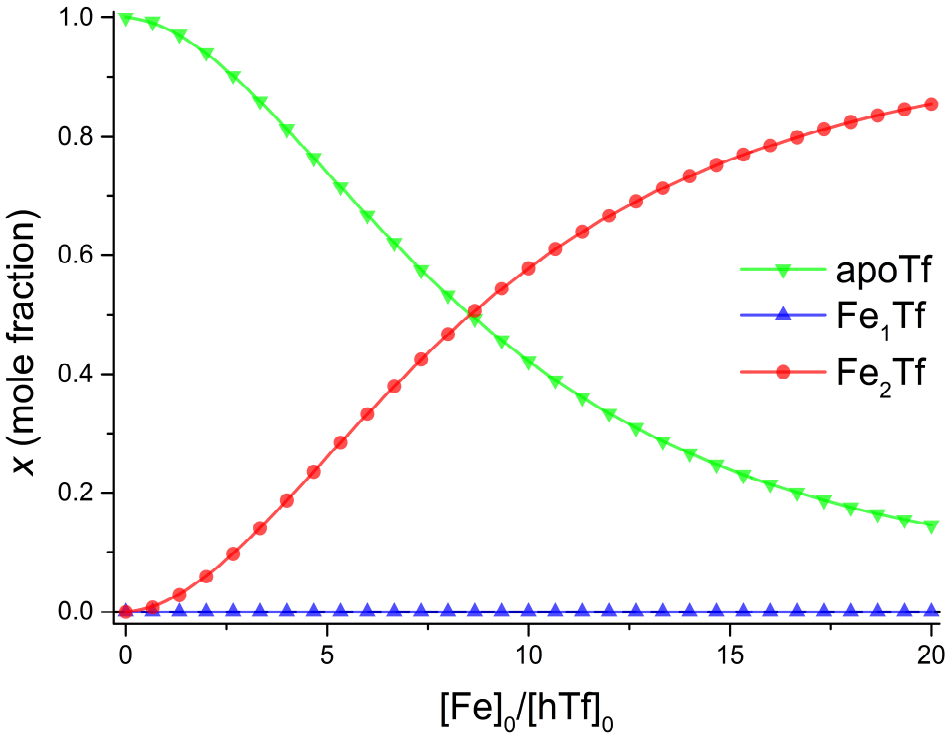

Figure S22. Transferrin speciation related to experiment presented in Figure S20 according to Eqs. 9-11 in the manuscript.

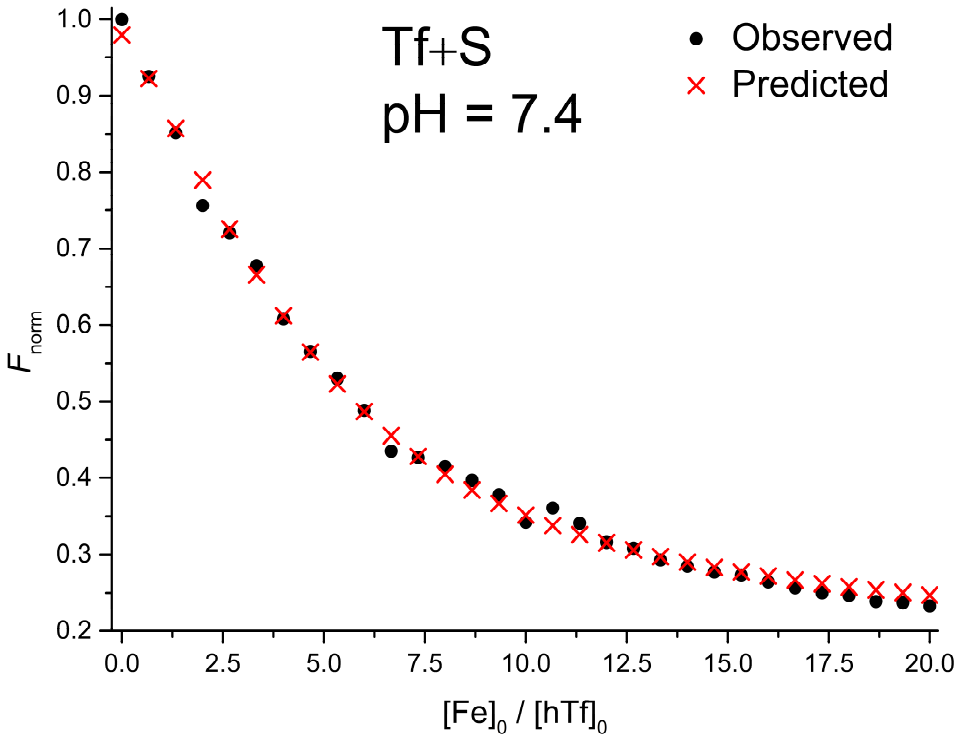

Figure S23. Measured (F_{obs}) and calculated (F_{calc}) normalized fluorescence for the spectrofluorometric titration of human serum transferrin (Tf+S) with FeNTA: $[hTf]_0$ = 2.11 µM, [PIPES] = 25 mM, [KCl] = 0.2 M, $[HCO_3^-]$ = 10 mM, $[NTA]_0$ = 50 mM, pH = 7.4, 25 °C. The parameters determined with the Solver tool in Microsoft Excel for the calculation of F_{calc} are: $\log(K_{1m})$ = 5.011 ± 0.016, $\log(R)$ = −0.233 ± 0.018, R^2 = 0.9970.

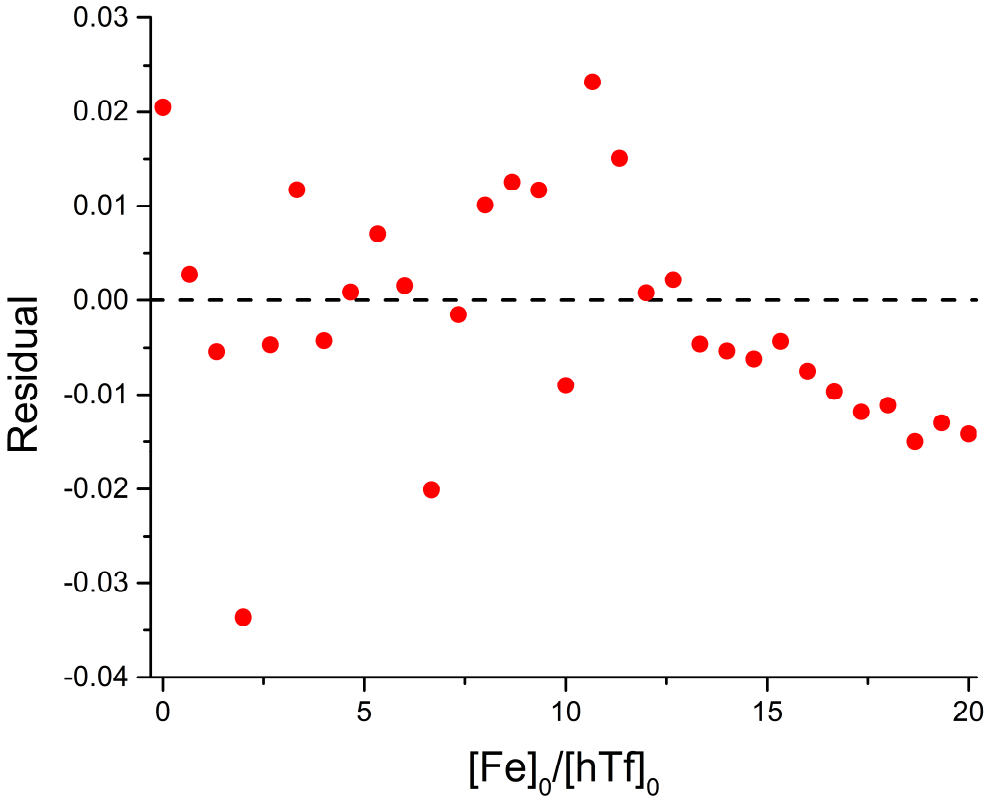

Figure S24. Residuals of fit related to experiment presented in Figure S23 calculated as $F_{calc} - F_{obs}$.

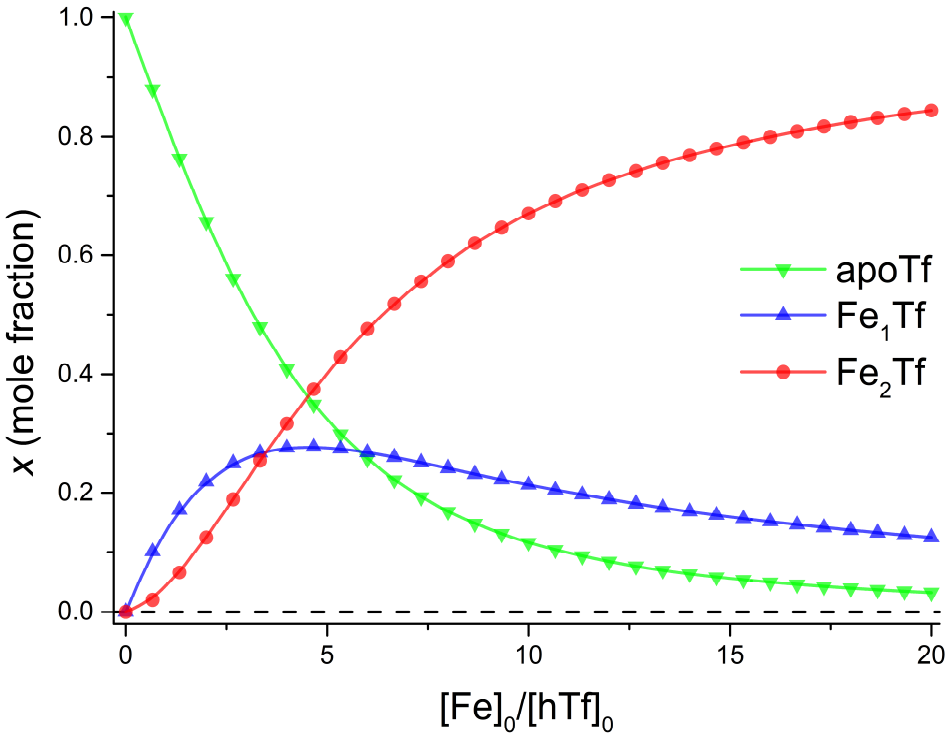

Figure S25. Transferrin speciation related to experiment presented in Figure S23 according to Eqs. 9-11 in the manuscript.

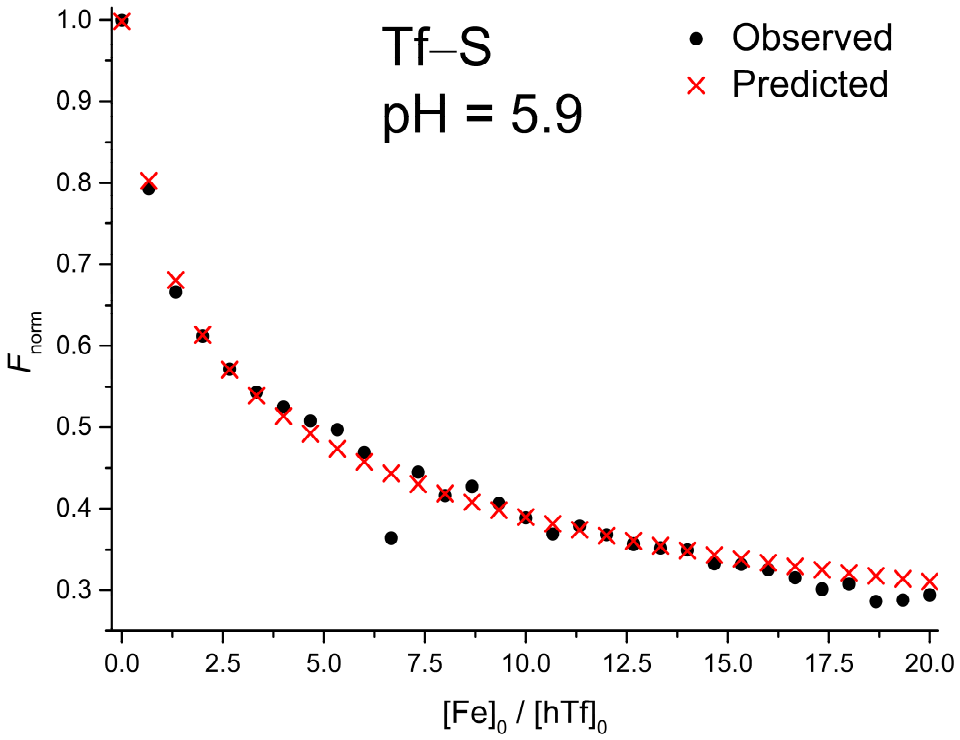

Figure S26. Measured (F_{obs}) and calculated (F_{calc}) normalized fluorescence for the spectrofluorometric titration of desialylated human serum transferrin (Tf–S) with FeNTA: $[hTf]_0$ = 1.70 µM, [PIPES] = 25 mM, [KCl] = 0.2 M, $[HCO_3^-]$ = 10 mM, $[NTA]_0$ = 0.1 mM, pH = 5.9, 25 °C. The parameters determined with the Solver tool in Microsoft Excel for the calculation of F_{calc} are: $\log(K_{1m})$ = 6.425 ± 0.049, $\log(R)$ = 1.569 ± 0.041, R^2 = 0.9863.

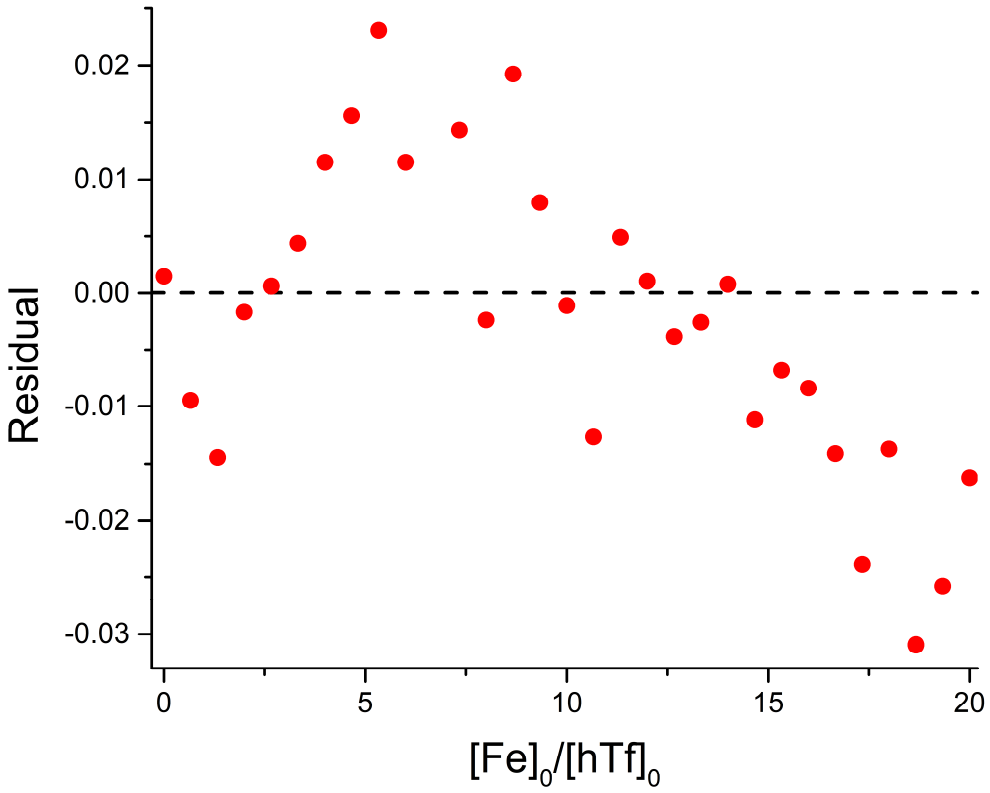

Figure S27. Residuals of fit related to experiment presented in Figure S26 calculated as $F_{calc} - F_{obs}$.

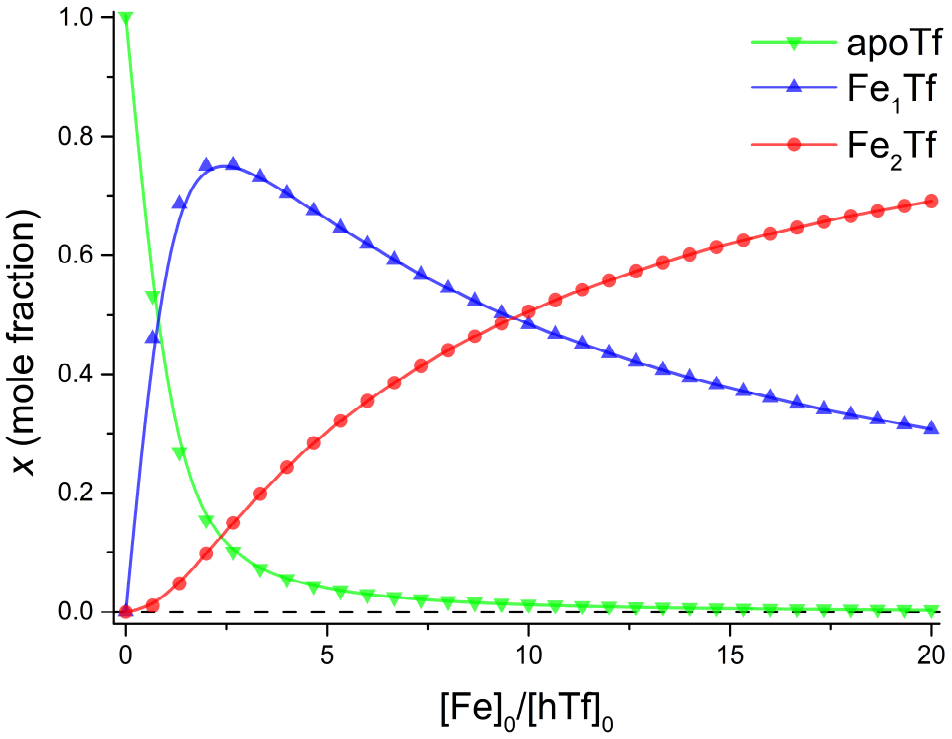

Figure S28. Transferrin speciation related to experiment presented in Figure S26 according to Eqs. 9-11 in the manuscript.

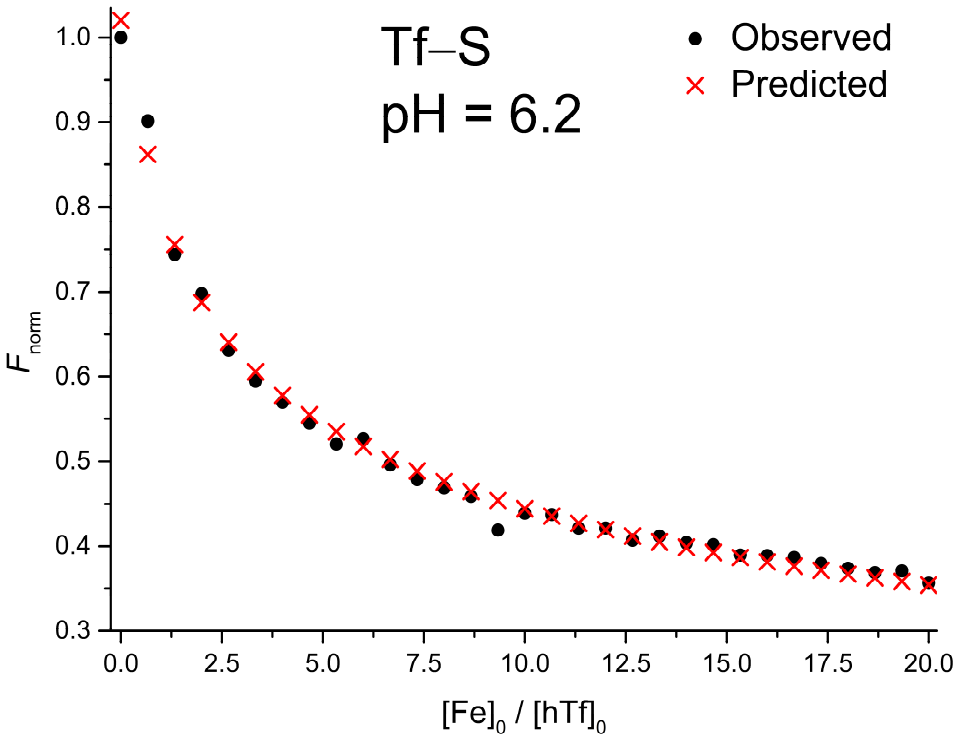

Figure S29. Measured (F_{obs}) and calculated (F_{calc}) normalized fluorescence for the spectrofluorometric titration of desialylated human serum transferrin (Tf–S) with FeNTA: $[hTf]_0$ = 1.60 µM, [PIPES] = 25 mM, [KCl] = 0.2 M, $[HCO_3^-]$ = 10 mM, $[NTA]_0$ = 0.5 mM, pH = 6.2, 25 °C. The parameters determined with the Solver tool in Microsoft Excel for the calculation of F_{calc} are: $\log(K_{1m})$ = 6.141 ± 0.160, $\log(R)$ = 1.406 ± 0.109, R^2 = 0.9930.

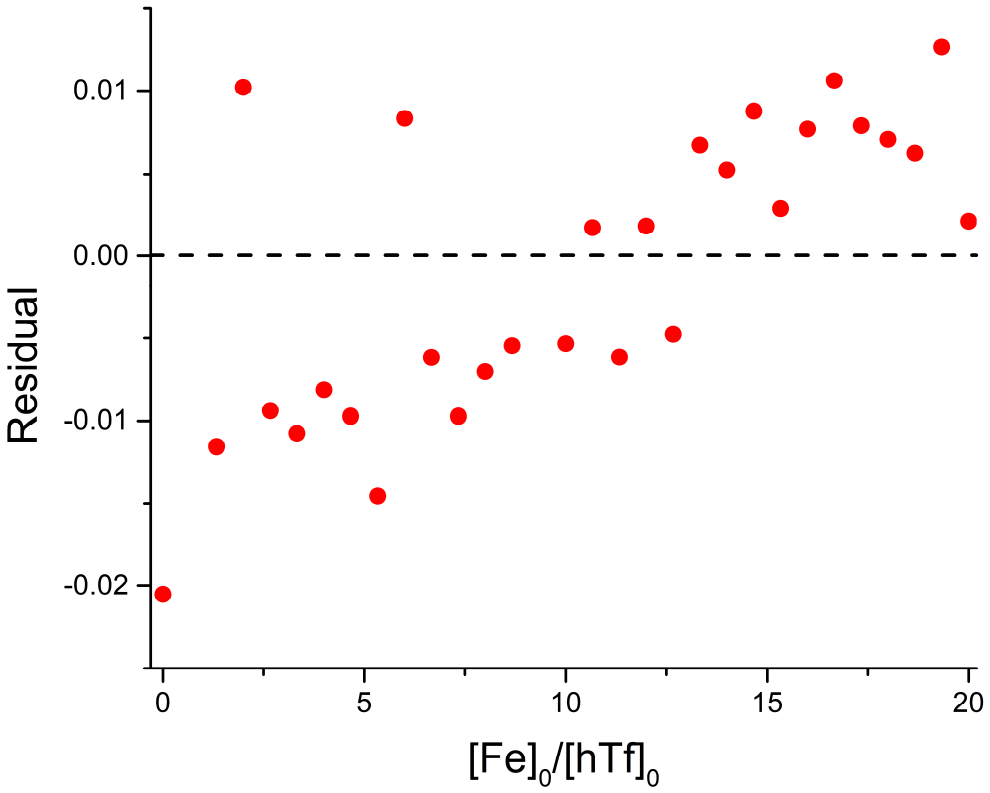

Figure S30. Residuals of fit related to experiment presented in Figure S29 calculated as $F_{calc} - F_{obs}$.

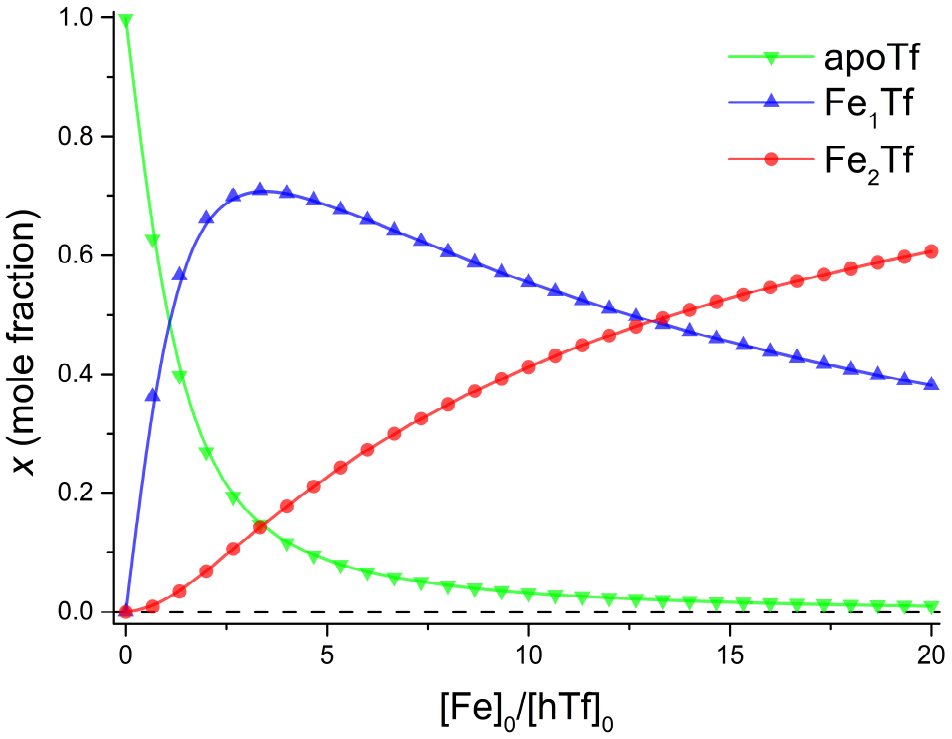

Figure S31. Transferrin speciation related to experiment presented in Figure S29 according to Eqs. 9-11 in the manuscript.

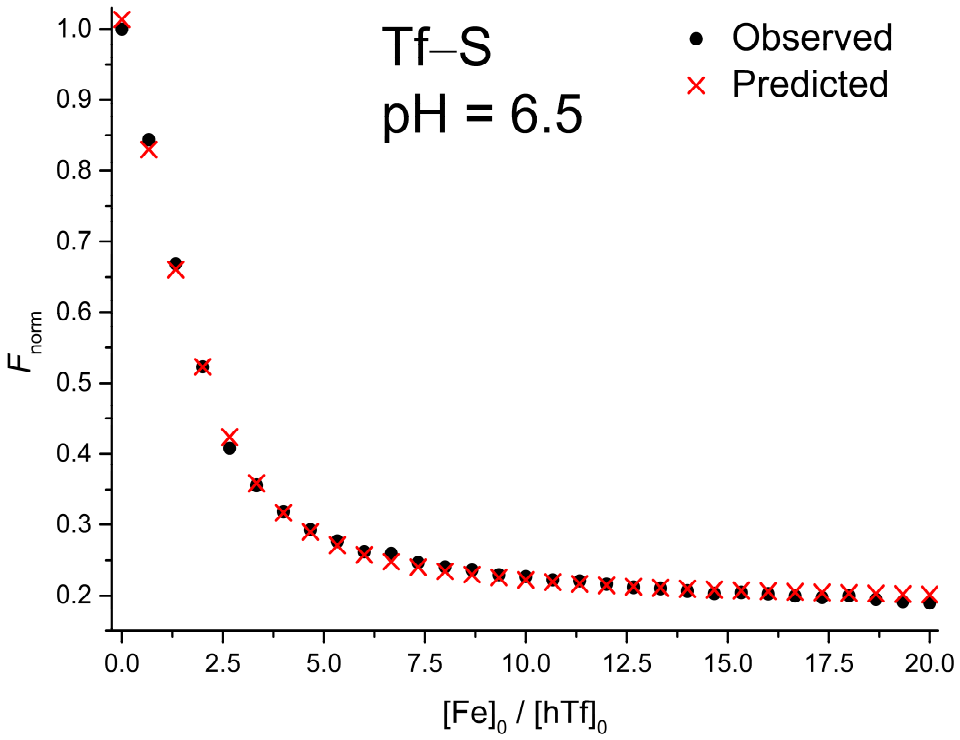

Figure S32. Measured (F_{obs}) and calculated (F_{calc}) normalized fluorescence for the spectrofluorometric titration of desialylated human serum transferrin (Tf–S) with FeNTA: $[hTf]_0$ = 1.61 µM, [PIPES] = 25 mM, [KCl] = 0.2 M, $[HCO_3^-]$ = 10 mM, $[NTA]_0$ = 0.5 mM, pH = 6.5, 25 °C. The parameters determined with the Solver tool in Microsoft Excel for the calculation of F_{calc} are: $\log(K_{1m})$ = 6.090 ± 0.031, $\log(R)$ = 0.136 ± 0.027, R^2 = 0.9987.

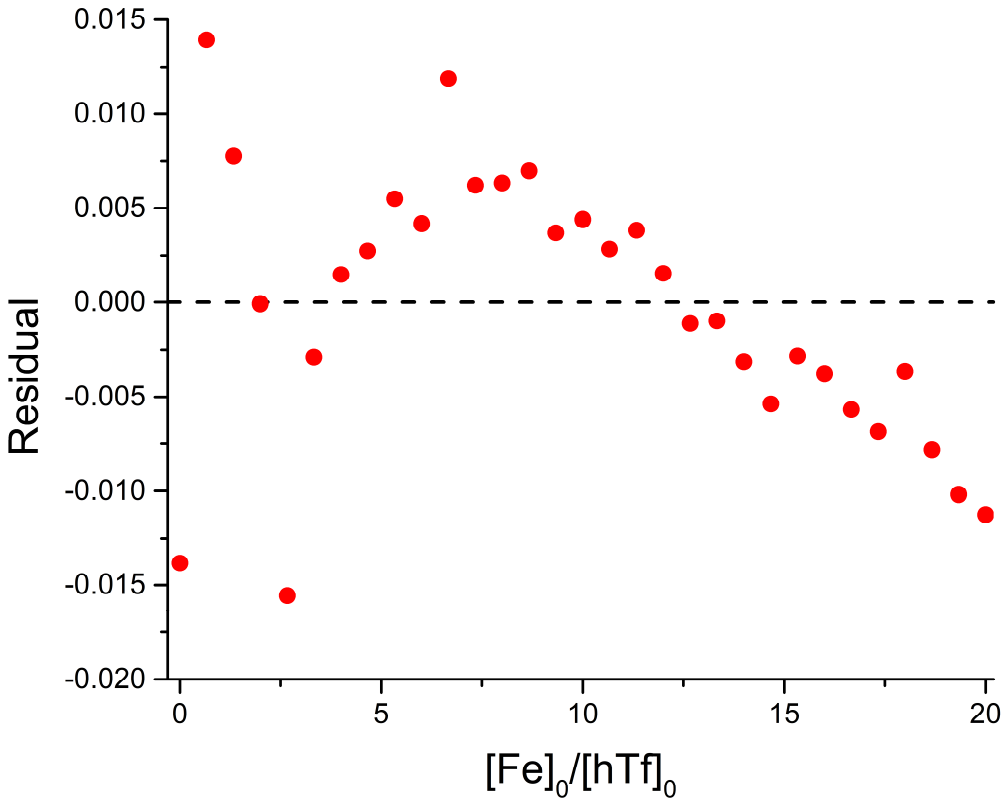

Figure S33. Residuals of fit related to experiment presented in Figure S32 calculated as $F_{calc} - F_{obs}$.

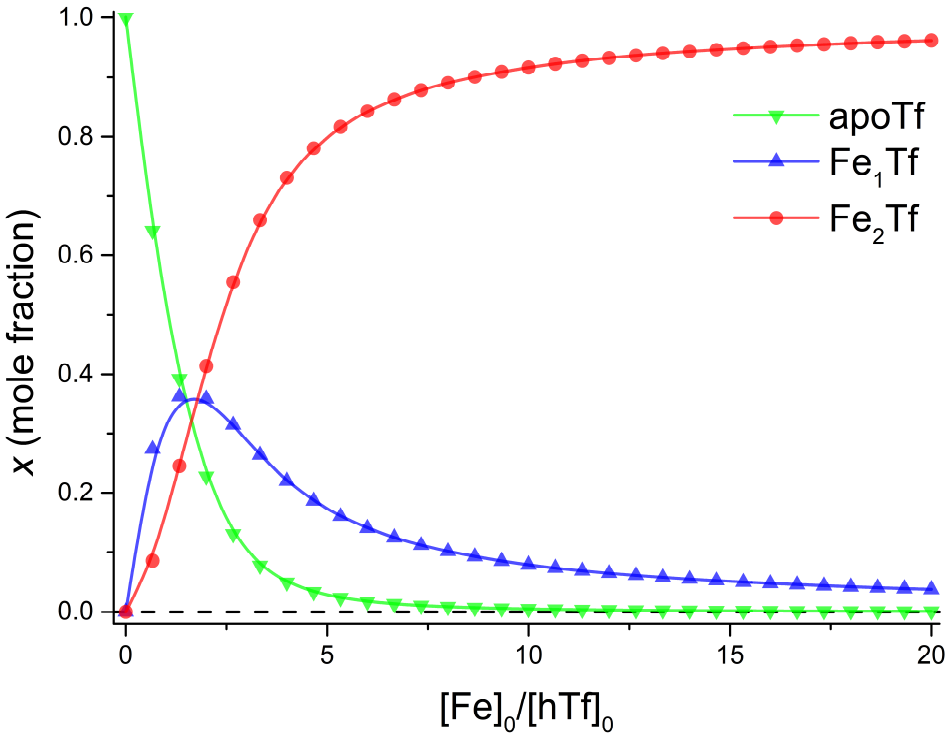

Figure S34. Transferrin speciation related to experiment presented in Figure S32 according to Eqs. 9-11 in the manuscript.

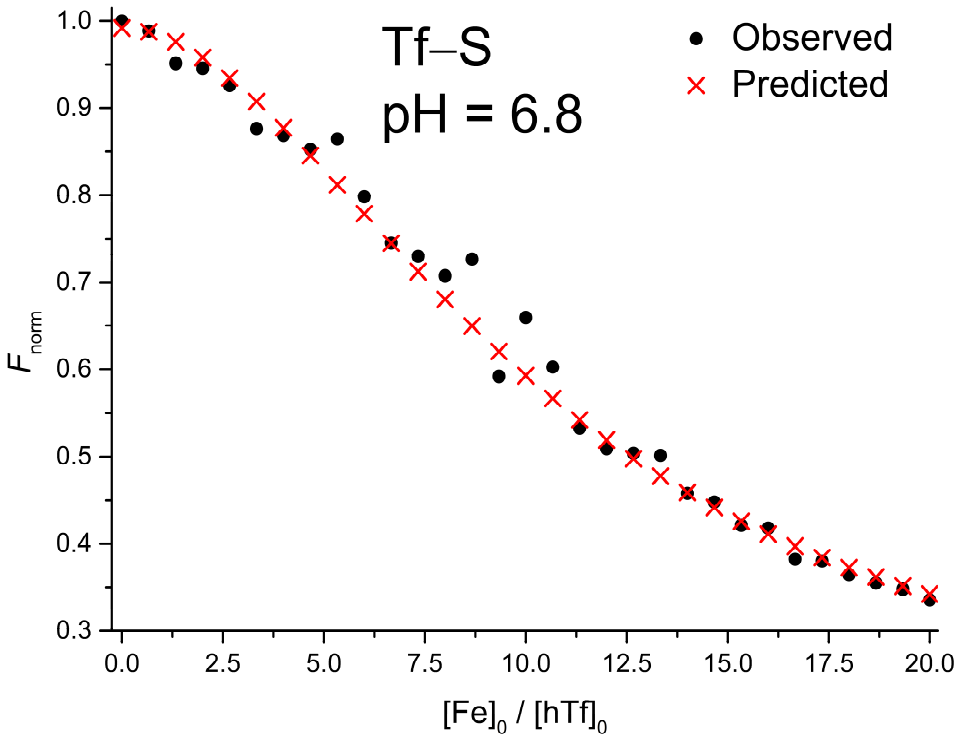

Figure S35. Measured (F_{obs}) and calculated (F_{calc}) normalized fluorescence for the spectrofluorometric titration of desialylated human serum transferrin (Tf–S) with FeNTA: $[hTf]_0$ = 3.84 µM, [PIPES] = 25 mM, [KCl] = 0.2 M, $[HCO_3^-]$ = 10 mM, $[NTA]_0$ = 10 mM, pH = 6.8, 25 °C. The parameters determined with the Solver tool in Microsoft Excel for the calculation of F_{calc} are: $\log(K_{1m})$ = 0.079 ± 0.041, $\log(R)$ = −9.504 ± 0.085, R^2 = 0.9873. At pH = 6.8, the calculated $\log(K_{1m})$ and $\log(R)$ are not meaningful because the second iron ion binding event may dominate and possibly mask the effects of the first binding event, leading to incorrect values of the equilibrium constant.

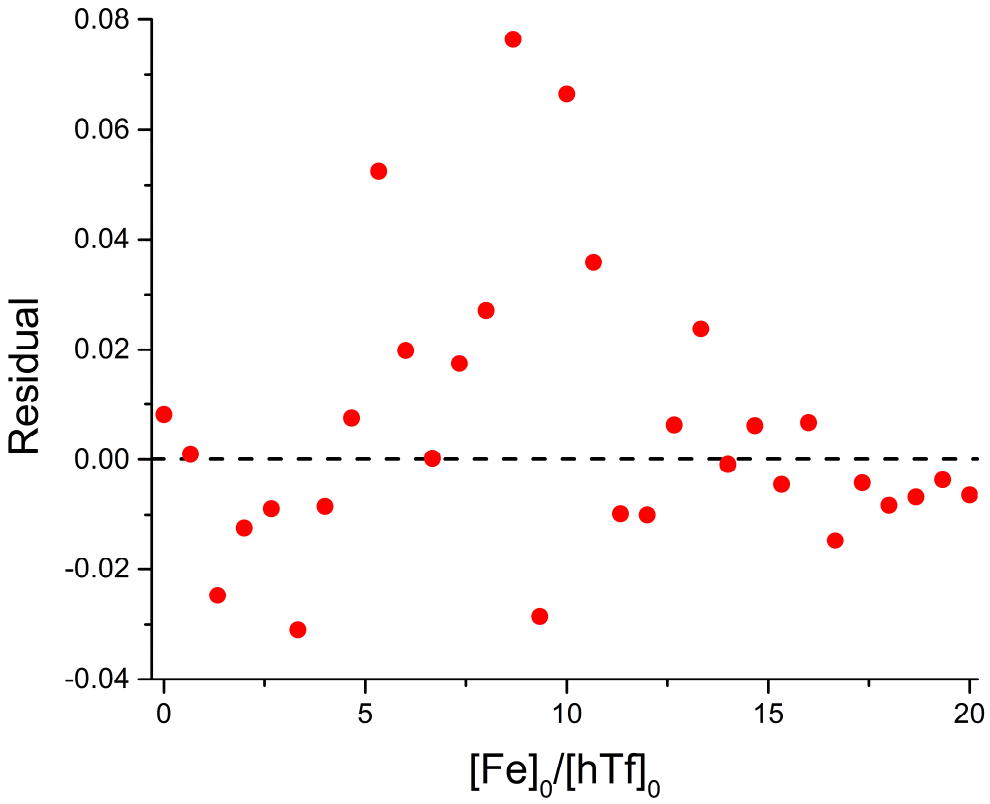

Figure S36. Residuals of fit related to experiment presented in Figure S35 calculated as $F_{calc} - F_{obs}$.

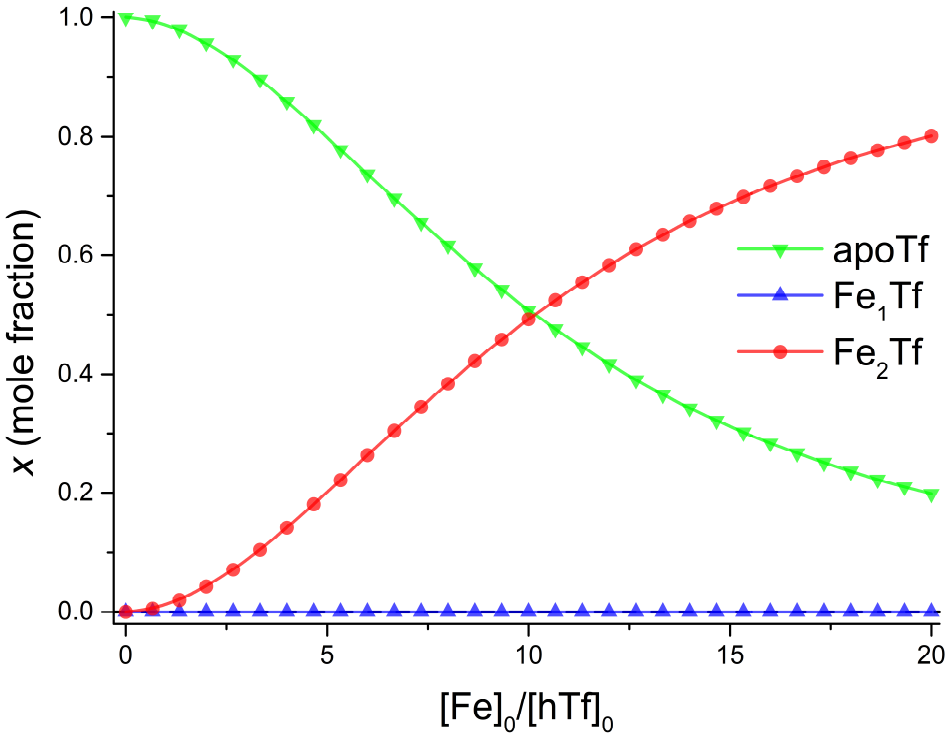

Figure S37. Transferrin speciation related to experiment presented in Figure S35 according to Eqs. 9-11 in the manuscript.

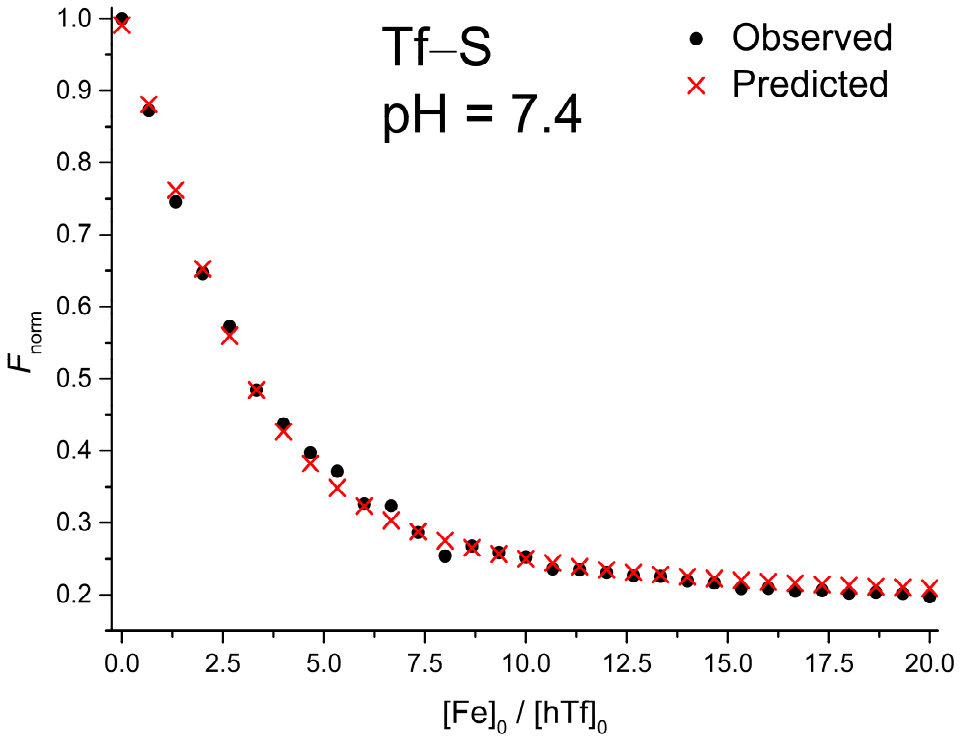

Figure S38. Measured (F_{obs}) and calculated (F_{calc}) normalized fluorescence for the spectrofluorometric titration of desialylated human serum transferrin (Tf–S) with FeNTA: $[hTf]_0$ = 1.54 µM, [PIPES] = 25 mM, [KCl] = 0.2 M, $[HCO_3^-]$ = 10 mM, $[NTA]_0$ = 50 mM, pH = 7.4, 25 °C. The parameters determined with the Solver tool in Microsoft Excel for the calculation of F_{calc} are: $\log(K_{1m})$ = 5.513 ± 0.025, $\log(R)$ = −0.260 ± 0.025, R^2 = 0.9977.

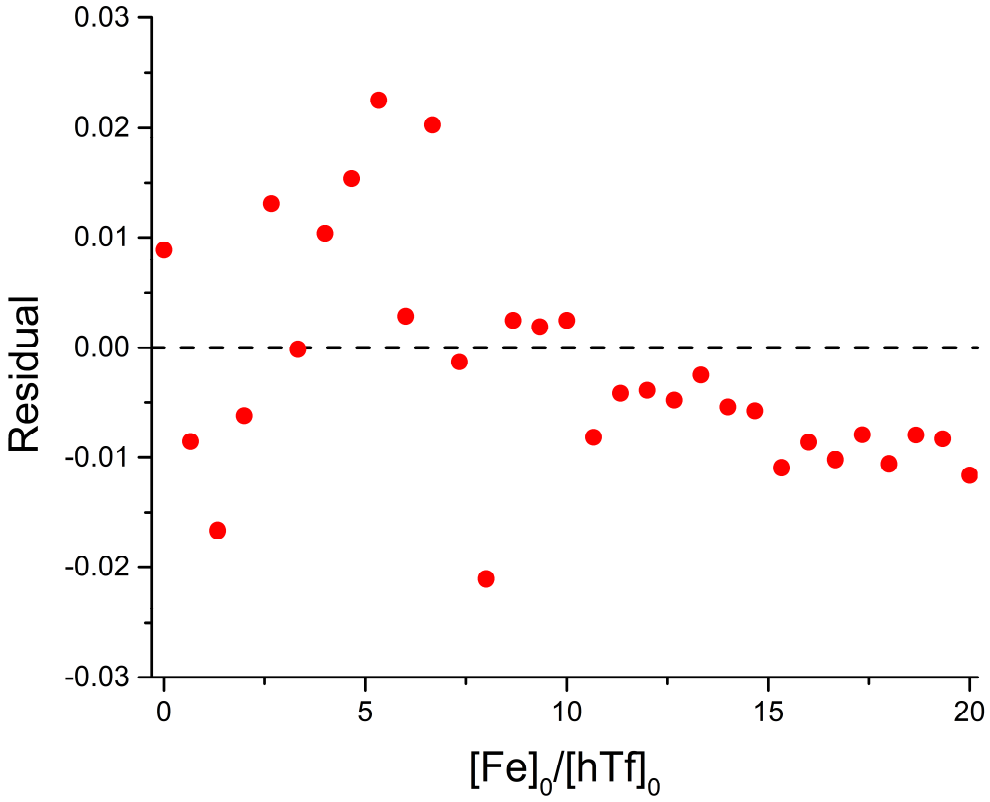

Figure S39. Residuals of fit related to experiment presented in Figure S38 calculated as $F_{calc} - F_{obs}$.

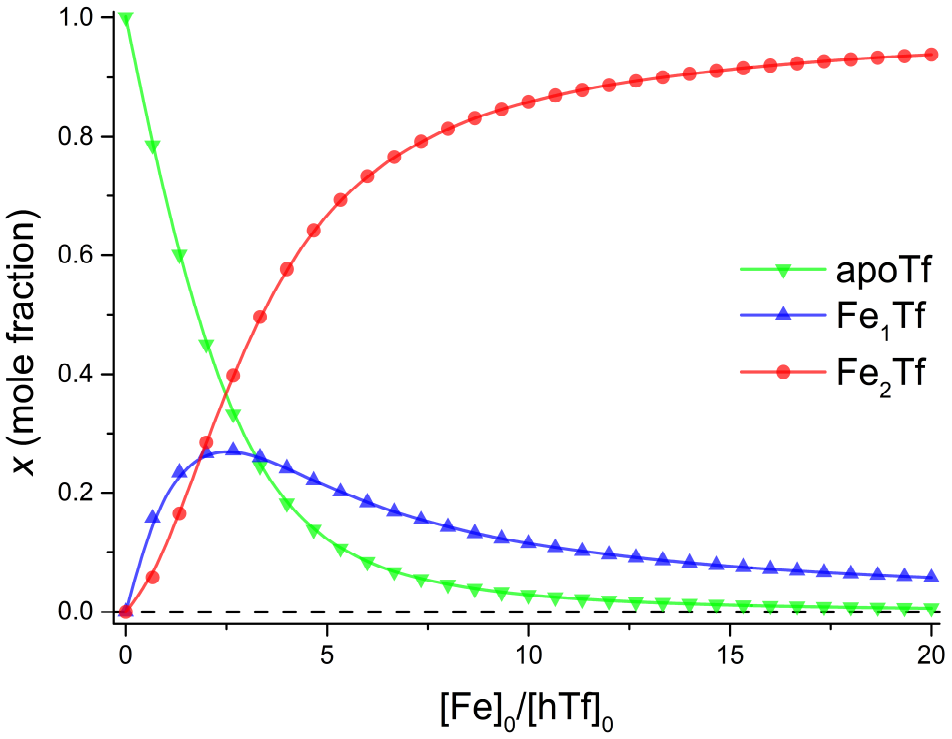

Figure S40. Transferrin speciation related to experiment presented in Figure S38 according to Eqs. 9-11 in the manuscript.

5.4. List of abbreviations

The abbreviations used in this subsection are as follows.

$\log(K_{1m})$ and $\log(K_{2m})$ are logarithmic values of the apparent binding (association) constants K_{1m} and K_{2m} for binding sites 1 and 2, respectively, as defined by Eqs. 3 and 4 in the manuscript (see also Subsection 7.1 in this document).

$\log(R)$ is the logarithmic value of the ratio K_{2m}/K_{1m}. Instead of fitting independent nominal values of the binding constants, the values of $\log(K_{1m})$ and $\log(R)$ were fitted, and the corresponding value of K_{2m} was calculated as $\log(K_{2m}) = \log(K_{1m}) + \log(R)$ (see also Subsection 7.2 of this document).

σ represents the standard deviations of the reported parameters. Details on error propagation can be found in Subsection 7.3 of this document.

R^2 is the coefficient of determination which quantifies the proportion of the variance in the dependent variable that is explained by the independent variable(s) in a regression model.

RSS represents the sum of the squared differences between the observed values (the actual data points) and the predicted values (the values estimated by the regression model).

F(FeTf) is the fractional population of the intermediate complex at half saturation defined by Eq. 19 in the manuscript.

K'_{110} is the pH-dependent conditional constant for the reaction of iron(III) with NTA.

$[NTA]_0$ / M represents fixed concentration of the NTA species within the titration.

Table S3. Output for titrations of native hTf (Tf+S) with FeNTA with carbonate as synergistic anion (25 mM PIPES, 10 mM K_2CO_3, 0.2 M KCl) obtained with the VBA routine for cubic equations with the coefficients given in Eqs. 6-8 in the manuscript using the Jenkins-Traub algorithm in Microsoft Excel 365 (Version 2304, build 16.0.16327.20200, 64-bit).[9–12]

pH	log(K_{1m})	σ	log(R)	σ	log(K_{2m})	σ	R^2	RSS	F(FeTf)	σ	K'_{110}	[NTA]$_0$ / M
7.4	5.011	0.016	−0.233	0.018	5.244	0.008	0.99695	0.00033	0.277	0.002	16.50	0.050
6.8[a]	0.001	<0.001	−9.531	0.013	9.532	0.014	0.99707	0.00053	<0.001	<0.001	15.30	0.010
6.5	5.886	0.032	1.175	0.022	4.711	0.012	0.99375	0.00018	0.659	0.006	14.70	0.0005
6.2	5.809	0.065	1.520	0.041	4.289	0.025	0.99601	0.00021	0.742	0.009	14.11	0.0005
5.9	5.425	0.012	1.541	0.008	3.884	0.007	0.99126	0.00016	0.747	0.001	13.51	0.0001

[a] At pH = 6.8, the calculated log(K_{1m}) and log(R) are not meaningful because the second iron ion binding event may dominate and possibly mask the effects of the first binding event, leading to incorrect values of the equilibrium constant.

Table S4. Output for titrations of desialylated hTf (Tf−S) with FeNTA with carbonate as synergistic anion (25 mM PIPES, 10 mM K_2CO_3, 0.2 M KCl) obtained with the VBA routine for cubic equations with the coefficients given in Eqs. 6-8 in the manuscript using the Jenkins-Traub algorithm in Microsoft Excel 365 (Version 2304, build 16.0.16327.20200, 64-bit).[9–12]

pH	log(K_{1m})	σ	log(R)	σ	log(K_{2m})	σ	R^2	RSS	F(FeTf)	σ	K'_{110}	[NTA]$_0$ / M
7.4	5.512	0.025	−0.261	0.025	5.773	0.008	0.99769	0.00012	0.270	0.004	16.50	0.050
6.8[a]	0.106	0.042	−9.456	0.085	9.561	0.045	0.98731	0.00085	<0.001	<0.001	15.30	0.010
6.5	6.089	0.031	0.135	0.027	5.954	0.009	0.99866	0.00021	0.369	0.006	14.70	0.0005
6.2	6.127	0.160	1.392	0.109	4.735	0.055	0.99301	0.00071	0.713	0.025	14.11	0.0005
6.2[b]	6.110	0.014	1.379	0.012	4.731	0.010	0.99319	0.00073	0.710	0.001	14.11	0.0005
5.9	6.421	0.049	1.564	0.041	4.857	0.011	0.98627	0.00044	0.752	0.008	13.51	0.0001

[a] At pH = 6.8, the calculated log(K_{1m}) and log(R) are not meaningful because the second iron ion binding event may dominate and possibly mask the effects of the first binding event, leading to incorrect values of the equilibrium constant.

[b] Values obtained omitting a single-point outlier from analysis.

6. Equilibria in the FeNTA solutions

The equilibrium reactions[14] related to the dissociation of H_4NTA^+ (in aqueous solutions) are as follows:

$$H^+ + NTA^{3-} \rightleftarrows HNTA^{2-} \qquad \log(K_1) = 9.59 \qquad \text{Eq. S7}$$

$$H^+ + HNTA^{2-} \rightleftarrows H_2NTA^- \qquad \log(K_2) = 2.58 \qquad \text{Eq. S8}$$

$$H^+ + H_2NTA^- \rightleftarrows H_3NTA \qquad \log(K_3) = 1.47 \qquad \text{Eq. S9}$$

$$H^+ + H_3NTA \rightleftarrows H_4NTA^+ \qquad \log(K_4) = 1.00 \qquad \text{Eq. S10}$$

The cumulative concentrations of all NTA species in the solution can be expressed as follows:

$$[NTA]_{total} = [H_4NTA^+] + [H_3NTA] + [H_2NTA^-] + [HNTA^{2-}] + [NTA^{3-}] \qquad \text{Eq. S11}$$

The coefficient[13] α^{-1} for the species NTA^{3-} can be represented as the ratio of $[NTA]_{total}$ to $[NTA^{3-}]$:

$$\alpha^{-1}(NTA^{3-}) = \frac{[NTA]_{total}}{[NTA^{3-}]} \qquad \text{Eq. S12}$$

$$= 1 + [H^+]K_1 + [H^+]^2 K_1 K_2 + [H^+]^3 K_1 K_2 K_3 + [H^+]^4 K_1 K_2 K_3 K_4$$

The following chemical equilibria[14,15] are valid for iron and NTA species in aqueous solutions:

$$Fe^{3+} + NTA^{3-} \rightleftarrows FeNTA \qquad \log(K_{110}) = 15.9 \qquad \text{Eq. S13}$$

$$FeNTA + NTA^{3-} \rightleftarrows Fe(NTA)_2{}^{3-} \qquad \log(K_{120}) = 8.07 \qquad \text{Eq. S14}$$

$$FeNTA \rightleftarrows Fe(OH)NTA^- + H^+ \qquad \log(K_{11-1}) = -4.36 \qquad \text{Eq. S15}$$

$$Fe(OH)NTA^- \rightleftarrows Fe(OH)_2NTA^{2-} + H^+ \qquad \log(K_{11-2}) = -7.58 \qquad \text{Eq. S16}$$

$$Fe(OH)_2NTA^{2-} \rightleftarrows Fe(OH)_3NTA^{3-} + H^+ \qquad \log(K_{11-3}) = -10.72 \qquad \text{Eq. S17}$$

$$2\,FeNTA + 2\,H_2O \rightleftarrows (Fe(OH)NTA)_2{}^{2-} + 2\,H^+ \qquad \log(K_{22-2}) = -6.0 \qquad \text{Eq. S18}$$

The total concentration of iron bound in all complexes with NTA ($[FeNTA]_{total}$) can be expressed as the sum of the individual concentrations of the iron-NTA species:

$$[FeNTA]_{total} = [FeNTA] + [Fe(NTA)_2{}^{3-}] + [Fe(OH)NTA^-] + [Fe(OH)_2NTA^{2-}] \qquad \text{Eq. S19}$$
$$+[Fe(OH)_3NTA^{3-}] + 2\left[(Fe(OH)NTA)_2{}^{2-}\right]$$

The coefficient α^{-1} for the FeNTA species (Eq. S12) can be determined by calculating the ratio of $[FeNTA]_{total}$ to [FeNTA]:

$$\alpha^{-1}(FeNTA) = \frac{[FeNTA]_{total}}{[FeNTA]} = 1 + K_{120}[NTA^{3-}] + \frac{K_{11-1}}{[H^+]} + \frac{K_{11-1}K_{11-2}}{[H^+]^2}$$
$$+ \frac{K_{11-1}K_{11-2}K_{11-3}}{[H^+]^3} + 2\,\frac{K_{22-2}\,K_{110}\,[Fe^{3+}]\,[NTA^{3-}]}{[H^+]^2} \qquad \text{Eq. S20}$$

Since the second and last components of the equation are insignificant under the experimental conditions of this study[1], the above expression simplifies to:

$$\alpha^{-1\prime}(\mathrm{FeNTA}) = \frac{[\mathrm{FeNTA}]_{\mathrm{total}}}{[\mathrm{FeNTA}]} = 1 + \frac{K_{11-1}}{[\mathrm{H}^+]} + \frac{K_{11-1}K_{11-2}}{[\mathrm{H}^+]^2} + \frac{K_{11-1}K_{11-2}K_{11-3}}{[\mathrm{H}^+]^3} \qquad \text{Eq. S21}$$

where $\alpha^{-1\prime}$(FeNTA) is constant at a fixed pH.

The analytical concentration of all NTA-containing species (usually referred to as $[\mathrm{NTA}]_0$) can be written as follows:

$$[\mathrm{NTA}]_0 = [\mathrm{NTA}]_{\mathrm{total}} + [\mathrm{FeNTA}]_{\mathrm{total}} \qquad \text{Eq. S22}$$

For further consideration of transferrin equilibria in Section 7, the reciprocal values of the α^{-1} coefficient can be conveniently written as follows:

$$\alpha(\mathrm{NTA}) = \frac{1}{\alpha^{-1}(\mathrm{NTA}^{3-})} \qquad \text{Eq. S23}$$

$$\alpha'(\mathrm{FeNTA}) = \frac{1}{\alpha^{-1\prime}(\mathrm{FeNTA})} \qquad \text{Eq. S24}$$

7. Equilibrium constants

7.1. Apparent and conditional equilibrium constants

In all the following expressions, charges have been omitted for the sake of clarity. The binding of the iron(III) ion in the form of FeNTA to apoTf can be described as follows:

$$\mathrm{apoTf} + \mathrm{FeNTA} \leftrightarrows \mathrm{FeTf} + \mathrm{NTA} \qquad \text{Eq. S25}$$

This corresponds to an apparent equilibrium constant:

$$K_{1\mathrm{app.}} = \frac{[\mathrm{FeTf}]\,[\mathrm{NTA}]}{[\mathrm{apoTf}]\,[\mathrm{FeNTA}]} \qquad \text{Eq. S26}$$

At fixed pH, a conditional equilibrium constant[13] can be defined:

$$K'_{1\mathrm{app.}} = \frac{[\mathrm{FeTf}]\,[\mathrm{NTA}]_{\mathrm{total}}}{[\mathrm{apoTf}]\,[\mathrm{FeNTA}]_{\mathrm{total}}} \qquad \text{Eq. S27}$$

where $[\mathrm{NTA}]_{\mathrm{total}}$ and $[\mathrm{FeNTA}]_{\mathrm{total}}$ are defined in Eqs. S11 and S19, respectively.

By combining Eq. S13 with S23 and S24, a pH-dependent conditional equilibrium constant for the association of Fe and NTA can also be formulated as follows:

$$K'_{110} = \frac{[\mathrm{FeNTA}]_{\mathrm{total}}}{[\mathrm{Fe}]\,[\mathrm{NTA}]_{\mathrm{total}}} = \frac{[\mathrm{FeNTA}]\,\alpha(\mathrm{NTA})}{[\mathrm{Fe}][\mathrm{NTA}]\,\alpha'(\mathrm{FeNTA})} = \frac{K_{110}\alpha(\mathrm{NTA})}{\alpha'(\mathrm{FeNTA})} \qquad \text{Eq. S28}$$

The Eq. S28 can be rearranged to:

$$\frac{[\mathrm{NTA}]_{\mathrm{total}}}{[\mathrm{FeNTA}]_{\mathrm{total}}} = \frac{\alpha'(\mathrm{FeNTA})}{[\mathrm{Fe}]\,K_{110}\,\alpha(\mathrm{NTA})} \qquad \text{Eq. S29}$$

The interaction between the unbound iron(III) ion and apoTf can be described as:

$$\mathrm{Fe} + \mathrm{apoTf} \leftrightarrows \mathrm{FeTf} \qquad \text{Eq. S30}$$

The corresponding equilibrium constant is defined as follows:

$$K'_{1\mathrm{m}} = \frac{[\mathrm{FeTf}]}{[\mathrm{Fe}]\,[\mathrm{apoTf}]} \qquad \text{Eq. S31}$$

Substituting Eq. S29 into Eq. S27 and combining with Eq. S31 gives:

$$K'_{1\mathrm{app.}} = \frac{K'_{1\mathrm{m}}\,\alpha'(\mathrm{FeNTA})}{K_{110}\,\alpha(\mathrm{NTA})} \qquad \text{Eq. S32}$$

The conditional equilibrium constant for the binding of the first iron(III) ion to apoTf can then be expressed as follows:

$$K'_{1\mathrm{m}} = K'_{1\mathrm{app.}}\, K'_{110} \qquad \text{Eq. S33}$$

The logarithmic representation of Eq. S33 is as follows:

$$\log(K'_{1\mathrm{m}}) = \log\left(K'_{1\mathrm{app.}}\right) + \log(K'_{110}) \qquad \text{Eq. S34}$$

The expression for the binding of the second iron(III) ion in the form of FeNTA to FeTf can be written as follows:

$$\mathrm{FeTf} + \mathrm{FeNTA} \leftrightarrows \mathrm{Fe_2Tf} + \mathrm{NTA} \qquad \text{Eq. S35}$$

The corresponding conditional equilibrium constant (similar to Eq. S27) can be written as follows:

$$K'_{2\mathrm{app.}} = \frac{[\mathrm{Fe_2Tf}]\,[\mathrm{NTA}]_{\mathrm{total}}}{[\mathrm{FeTf}]\,[\mathrm{FeNTA}]_{\mathrm{total}}} \qquad \text{Eq. S36}$$

Similar to Eq. S30, the binding of the unbound iron(III) ion to FeTf can be written as follows:

$$\mathrm{Fe} + \mathrm{FeTf} \leftrightarrows \mathrm{Fe_2Tf} \qquad \text{Eq. S37}$$

This corresponds to an equilibrium constant:

$$K'_{2m} = \frac{[\mathrm{Fe_2Tf}]}{[\mathrm{Fe}]\,[\mathrm{FeTf}]} \qquad \text{Eq. S38}$$

Again, substituting Eq. S29 into Eq. S36 and combining with Eq. S38 gives the following:

$$K'_{2\mathrm{app.}} = \frac{K'_{2\mathrm{m}}\,\alpha(\mathrm{FeNTA})}{K_{110}\,\alpha(\mathrm{NTA})} \qquad \text{Eq. S39}$$

$$K'_{2\mathrm{m}} = K'_{2\mathrm{app.}}\, K'_{110} \qquad \text{Eq. S40}$$

$$\log K'_{2\mathrm{m}} = \log K'_{2\mathrm{app.}} + \log K'_{110} \qquad \text{Eq. S41}$$

As Harris and Pecoraro have noted[16], the values of $K'_{1\mathrm{m}}$ and $K'_{2\mathrm{m}}$ are conditional constants, valid only for a given pH of the solution and a given HCO_3^- concentration.

7.2. Data fitting

The concentration of free iron (Eq. 5 in the manuscript) was calculated for each data point with the initial values of $\log(K_{1m})$ and $\log(R)$ using the VBA cubic equation routine (with the coefficients from Eqs. 6-8 in the manuscript) using the Jenkins-Traub algorithm in Microsoft Excel 365 (version 2304, build 16.0.16327.20200, 64-bit).[17–20] The differences $F_{calc} - F_{norm}$ were squared and summed for all data points to obtain the residual sum of squares (RSS). Inverse-variance weighting ($1/\sigma^2$, where σ^2 is the variance of the fluorescence measurements in triplicate) was used to calculate the RSS value to optimize the accuracy of the fitting process. This approach effectively minimizes the impact of random errors in the dataset and ensures that the fitting algorithm highlights the most reliable and reproducible data points. The RSS value was then minimized through an iterative procedure to obtain the optimal set of binding constants using the solver tool in Microsoft Excel.

Several strategies were used to improve the convergence of the fit: (i) normalized fluorescence values were used instead of raw values, (ii) instead of fitting independent nominal values of the binding constants, the values of $\log(K_{1m})$ and $\log(R)$ were fitted, and the corresponding value of K_{2m} was calculated as $\log(K_{2m}) = \log(K_{1m}) + \log(R)$, and (iii) the data were randomized before fitting. The values of $\log(K_{1m})$ were used to ensure positive non-zero values of K_{1m}. Randomization of data points was performed by calculating (pseudo-)random values using the function RAND() and sorting by the obtained values.

7.3. Error propagation

7.3.1. Fluorescence measurements

The standard deviation of the respective replicated (and baseline-corrected) fluorescence titration point was calculated by considering both the contributions of the standard deviation of the measured sample and the standard deviation of the baseline, as shown in Eqs. S42, S43, and S44.

$$s(F_{\mathrm{BASELINE-CORRECTED}})_i^{\,2} = s(F_{\mathrm{MEASURED}})_i^{\,2} + s(F_{\mathrm{BASELINE}})_i^{\,2} \qquad \text{Eq. S42}$$

$$s(F_{\mathrm{BASELINE-CORRECTED}})_i = \sqrt{s(F_{\mathrm{MEASURED}})_i^{\,2} + s(F_{\mathrm{BASELINE}})_i^{\,2}} \qquad \text{Eq. S43}$$

As mentioned previously, the fluorescence was IFE-corrected using the ZINFE method (F_Z, Eq. S5). The exponential term, which is a function of the geometric parameters, can be denoted as a single term N[4], as shown in Eq. S44:

$$F_Z = F_{0(z1)} \left(\frac{F_{0(z1)}}{F_{0(z2)}}\right)^N \qquad \text{Eq. S44}$$

The procedure for calculating the equilibrium constants requires the determination of weighting coefficients for fluorescence measurements. Since weighting factors with inverse variance are used for the fitting procedure, the variance of the IFE-corrected, baseline-corrected fluorescence must be estimated. To estimate the error of the IFE-corrected fluorescence, the partial derivatives were calculated according to Eqs. S45 and S46:

$$\frac{\partial F_Z(F_{0(z1)},F_{0(z2)},N)}{\partial F_{0(z1)}} = (N+1)\left(\frac{F_{0(z1)}}{F_{0(z2)}}\right)^N \qquad \text{Eq. S45}$$

$$\frac{\partial F_Z(F_{0(z1)},F_{0(z2)},N)}{\partial F_{0(z2)}} = -N\left(\frac{F_{0(z1)}}{F_{0(z2)}}\right)^{(1+N)} \qquad \text{Eq. S46}$$

$$\frac{\partial F_Z(F_{0(z1)},F_{0(z2)},N)}{\partial N} = F_{0(z1)}\left(\frac{F_{0(z1)}}{F_{0(z2)}}\right)^N \ln\left(\frac{F_{0(z1)}}{F_{0(z2)}}\right) \quad \text{Eq. S47}$$

The error of the exponent N results primarily from inaccuracies in the liquid height within the microplate well, since the internal geometrical parameters of the microplate reader, the dimensions of the microplate and the z-positions are precisely defined (*e.g.* the z-positions are specified with an accuracy of up to 1 µm). $F_{0(z1)}$ and $F_{0(z2)}$ represent fluorescence values measured at two different z-positions.

The variance, including the correlation, is determined as described in Eq. S48.

$$s_{F_Z}{}^2 = \left(\frac{\partial F_Z}{\partial F_{0(z1)}} s_{F_{0(z1)}}\right)^2 + \left(\frac{\partial F_Z}{\partial F_{0(z2)}} s_{F_{0(z2)}}\right)^2 + \left(\frac{\partial F_Z}{\partial N} s_N\right)^2$$

$$-2\mathrm{cov}\left(F_{0(z1)}, F_{0(z2)}\right)(N+1)N\left(\frac{F_{0(z1)}}{F_{0(z2)}}\right)^N\left(\frac{F_{0(z1)}}{F_{0(z2)}}\right)^{(1+N)} \quad \text{Eq. S48}$$

The standard deviation of the IFE-corrected fluorescence is calculated as the square root of the variance obtained by Eq. S48.

7.3.2. Equilibrium constants

The values of $\log(K_{1m})$ and $\log(R)$ were determined by iterative fitting while solving the equations for mass conservation, as described in the manuscript. The uncertainties in the fitting parameters $\log(K_{1m})$ and $\log(R)$ were determined using the "jackknife" method by omitting one data point at a time from the RSS calculation and fitting all remaining points to obtain a new set of parameters.[21] For each omitted titration point, $\log(K_{1m})$ and $\log(R)$ were determined, and the average value was calculated.

Standard deviations are first approximated using Eqs. S49 and S50:

$$s(K_{1m}) = \sqrt{\frac{1}{n-1}\sum_{i=1}^{n}(K_{1mi} - \bar{K}_{1m})} \quad \text{Eq. S49}$$

$$s(R) = \sqrt{\frac{1}{n-1}\sum_{i=1}^{n}(R_i - \bar{R})} \quad \text{Eq. S50}$$

Where K_{1mi} and R_i are i-th values of K_{1m} and R, n is the number of titration points used for the calculation.

The above expressions do not take into account the systematic errors resulting from the slight uncertainties in the concentrations of transferrin and FeNTA due to the uncertainties in their respective molar absorbance coefficients. Due to the difficulty in propagating the error through the iterative procedure, we performed a sensitivity analysis to assess the impact of concentration variations on the uncertainties of the calculated equilibrium constants.[22] Concentrations were adjusted to both higher (H) and lower (L) estimates, resulting in four scenarios: LL, LH, HL, HH. These adjustments are based on the addition or subtraction of one standard deviation from the average concentrations. "L" refers to the lower estimate of a concentration calculated by subtracting one standard deviation from the mean, while "H" refers to the higher estimate obtained by adding one standard deviation to the mean. K_{1m} and R were recalculated for each scenario across all titration points, expanding the data set by a factor of four.

Accordingly, the standard deviations were calculated using this (fourfold) extended data set. They were then rescaled to the original data set, assuming that the relative standard deviation remains consistent in both the extended and the original data set. Therefore, the reported K_{1m} and R values are based on the original, unadjusted concentrations, but the associated uncertainties were estimated as described above.

The K_{2m} is calculated as shown in Eq. S51.

$$K_{2m} = K_{1m}R \quad \text{Eq. S51}$$

Therefore, the error propagation for K_{2m} (including the covariance) is described in Eq. S52.

$$s(K_{2m}) = \sqrt{\left(\frac{\partial K_{2m}}{\partial K_{1m}}\right)^2 s(K_{1m})^2 + \left(\frac{\partial K_{2m}}{\partial R}\right)^2 s(R)^2 + 2\frac{\partial K_{2m}}{\partial K_{1m}}\frac{\partial K_{2m}}{\partial R}\mathrm{COV}(K_{1m}, R)} \quad \text{Eq. S52}$$

The partial derivatives are calculated as shown in the following equations:

$$\frac{\partial K_{2m}}{\partial K_{1m}} = R \quad \text{Eq. S53}$$

$$\frac{\partial K_{2m}}{\partial R} = K_{1m} \quad \text{Eq. S54}$$

For logarithmic transformations of: K_{1m}, R, K_{2m}, the uncertainties in their logarithmic expressions can be represented as shown below.

$$s(\log(X)) = \frac{s(X)}{\ln(10)X} \quad \text{Eq. S55}$$

where X represents either: K_{1m}, R, or K_{2m}.

From K_{1m} and K_{2m}, the conditional thermodynamic binding constants K'_{1m} and K'_{2m} are calculated as given in Eq. S56 and Eq. S57.

$$K'_{1m} = K_{1m}K'_{110} \quad \text{Eq. S56}$$

$$K'_{2m} = K_{2m}K'_{110} \quad \text{Eq. S57}$$

The error propagation is estimated as shown below.

$$s(K'_{1m}) = \sqrt{s^2(K_{1m}) + s^2(K'_{110})} \quad \text{Eq. S58}$$

$$s(K'_{2m}) = \sqrt{s^2(K_{2m}) + s^2(K'_{110})} \quad \text{Eq. S59}$$

The standard deviation for the logarithmically transformed pH-dependent conditional constant, $\log(K'_{110})$, is set to 0.01, as previously reported.[14,23]

7.3.3. Other calculations

Error propagation for the fractional population of the intermediate complex at 50% saturation, *F*(FeTf), defined by Eq. 19 in the manuscript, was performed using the following equations:

$$\frac{\partial F(\mathrm{FeTf})}{\partial K_{1\mathrm{m}}} = \frac{\partial\left(\frac{K_{1\mathrm{m}}}{2\sqrt{K_{1\mathrm{m}}K_{2\mathrm{m}}}+K_{1\mathrm{m}}}\right)}{\partial K_{1\mathrm{m}}} = \frac{\sqrt{K_{1\mathrm{m}}K_{2\mathrm{m}}}}{\left(2\sqrt{K_{1\mathrm{m}}K_{2\mathrm{m}}}+K_{1\mathrm{m}}\right)^2} \quad \text{Eq. S60}$$

$$\frac{\partial F(\mathrm{FeTf})}{\partial K_{2\mathrm{m}}} = \frac{\partial\left(\frac{K_{2\mathrm{m}}}{2\sqrt{K_{1\mathrm{m}}K_{2\mathrm{m}}}+K_{1\mathrm{m}}}\right)}{\partial K_{2\mathrm{m}}} = -\frac{{K_{1\mathrm{m}}}^2}{\sqrt{K_{1\mathrm{m}}K_{2\mathrm{m}}}\left(2\sqrt{K_{1\mathrm{m}}K_{2\mathrm{m}}}+K_{1\mathrm{m}}\right)^2} \quad \text{Eq. S61}$$

$$s(F(\mathrm{FeTf})) = \sqrt{\left(s(K_{1\mathrm{m}})\frac{\partial F(\mathrm{FeTf})}{\partial K_{1\mathrm{m}}}\right)^2 + \left(s(K_{2\mathrm{m}})\frac{\partial F(\mathrm{FeTf})}{\partial K_{2\mathrm{m}}}\right)^2 + 2\mathrm{COV}(K_{1\mathrm{m}}, K_{2\mathrm{m}})\frac{\partial F(\mathrm{FeTf})}{\partial K_{1\mathrm{m}}}\frac{\partial F(\mathrm{FeTf})}{\partial K_{2\mathrm{m}}}} \quad \text{Eq. S62}$$

Error propagation for the site preference factor f_{sp}, defined as $K_{1m}/K_{2m} = K'_{1m}/K'_{2m}$, was performed using the following equations:

$$\frac{\partial f_{\mathrm{sp}}}{\partial K_{1\mathrm{m}}} = \frac{1}{K_{2\mathrm{m}}} \quad \text{Eq. S63}$$

$$\frac{\partial f_{\mathrm{sp}}}{\partial K_{2\mathrm{m}}} = -\frac{K_{1\mathrm{m}}}{{K_{2\mathrm{m}}}^2} \quad \text{Eq. S64}$$

$$s(f_{\mathrm{sp}}) = \sqrt{\left(s(K_{1\mathrm{m}})\frac{\partial f_{\mathrm{sp}}}{\partial K_{1\mathrm{m}}}\right)^2 + \left(s(K_{2\mathrm{m}})\frac{\partial f_{\mathrm{sp}}}{\partial K_{2\mathrm{m}}}\right)^2 + 2\mathrm{COV}(K_{1\mathrm{m}}, K_{2\mathrm{m}})\frac{\partial f_{\mathrm{sp}}}{\partial K_{1\mathrm{m}}}\frac{\partial f_{\mathrm{sp}}}{\partial K_{2\mathrm{m}}}} \quad \text{Eq. S65}$$

8. Statistical analysis

For the *t*-test to work well, the data must fulfill the conditions of independence, normality, and homoscedasticity of errors. While it is known that the *t*-test is robust to small deviations from normality, it has been shown that heteroscedasticity, skewness, and outliers affect both the type I error and power. Therefore, a more robust Satterthwaite's approximate *t*-test was used when comparing the means of two independent groups with unequal variances. A conventional *t*-test assumes that the variances in both groups are equal. Satterthwaite's approach provides a more accurate and robust solution by estimating the degrees of freedom based on the sample variances of the two groups. This modification helps to account for the unequal variances and improves the validity of the *t*-test. By adjusting the degrees of freedom, Satterthwaite's approximate *t*-test ensures that the *p*-value and confidence intervals of the test are more accurate, leading to more reliable inferences about the population means.[24]

Specifically, the test statistic *d* is calculated as:

$$d = \frac{\bar{x}_1 - \bar{x}_2}{\sqrt{\frac{{s_1}^2}{n_1} + \frac{{s_2}^2}{n_2}}} \qquad \text{Eq. S66}$$

where $\bar{x}_1$ and $\bar{x}_2$ are the mean values of the parameters obtained from the measurements, $n_1 = n_2 = 3$ is the number of replicate measurements, and s_1^2 and s_2^2 are the variances of the parameters.

The approximate degrees of freedom are then calculated as follows:

$$df = \frac{\left[\frac{{s_1}^2}{n_1} + \frac{{s_2}^2}{n_2}\right]^2}{\frac{\left({s_1}^2/n_1\right)^2}{n_1 - 1} + \frac{\left({s_2}^2/n_1\right)^2}{n_2 - 1}} \qquad \text{Eq. S67}$$

Using the same values for *n* and s^2.

In the context of Satterthwaite's approximate *t*-test, the null hypothesis states that there is no significant difference between the mean values of the two independent groups to be compared. The obtained *p*-values correspond to the probability that the observed differences are due to random error only, and the values of $p \leq \alpha$ were determined to be statistically significant. The chosen significance level of $\alpha = 0.05$ means that there is a 5% risk of inferring a statistically significant difference, even though there is no actual difference (type I error).

Statistical significance of the observed differences is encoded as $p < 0.001$ (***), $p < 0.01$ (**), $p < 0.025$ (*), $p < 0.1$ (').

8.1. Satterthwaite's approximate *t*-test

Table S5. Summary of Satterthwaite's approximate *t*-test for the values of the conditional macroscopic constants (log(K_1'$_m$) and log(K_2'$_m$)). All values and calculated statistics are archived and available for reference.[25]

pH	log(K_1'$_m$)				log(K_2'$_m$)			
	d	*df*	*p*-value	significance	*d*	*df*	*p*-value	significance
7.4	26.3	3.59	<0.001	***	49.7	4.00	<0.001	***
6.8[a]	4.12	2.22	0.054	·	1.06	2.54	0.400	
6.5	7.50	4.00	0.002	**	105	3.98	<0.001	***
6.2[b]	3.17	2.64	0.087	·	12.4	3.00	0.001	**
5.9	32.9	2.41	<0.001	***	87.7	3.82	<0.001	***

[a] At pH = 6.8, the calculated log(K_{1m}) and log(R) are not meaningful because the second iron ion binding event may dominate and possibly mask the effects of the first binding event, leading to incorrect values of the equilibrium constant.

[b] If a significant single-point outlier is omitted from the titration of Tf−S, the following adjusted values result: d = 7.76, df = 2.27, p-value = 0.016205, significance = *, for log(K_1'$_m$) and: d = 25.2, df = 3.00, p-value = 0.000137, significance = ***, for log(K_2'$_m$).

Table S6. Summary of Satterthwaite's approximate *t*-test for the fractional population of the intermediate at half saturation (F(FeTf)). All values and calculated statistics are archived and are available for reference.[25]

pH	F(FeTf)			
	d	*df*	*p*-value	significance
7.4	2.71	2.94	0.113	
6.8[a]	0.00	4.00	1.000	*
6.5	59.2	4.00	<0.001	***
6.2[b]	1.89	2.51	0.199	
5.9	1.07	2.06	0.395	

[a] At pH = 6.8, the calculated log(K_{1m}) and log(R) are not meaningful because the second iron ion binding event may dominate and possibly mask the effects of the first binding event, leading to incorrect values of the equilibrium constant.

[b] If a significant single-point outlier is omitted from the titration of Tf−S, the following adjusted values result: d = 6.12, df = 2.05, p-value = 0.026, significance = *.

9. Additional information

Table S7. Results of the mathematical model of the observed pH-dependence of the binding constants, defined by Chasteen and Williams.[26] f_{sp} is the site preference factor defined as K_{1m}/K_{2m}

	Tf+S		Tf−S	
pH	f_{sp}	f_{sp} (simulated)	f_{sp}	f_{sp} (simulated)
7.4	0.58	0.58	0.55	0.55
6.5	15.0	15.0	1.36	1.36
6.2	33.1	33.1	24.7	24.7
5.9	34.8	34.8	36.6	36.6

[a] If a significant single-point outlier is omitted from the titration of Tf−S, the following adjusted values result: f_{sp} = 23.9, f_{sp} (simulated) = 23.9.

Table S8. Parameters of the mathematical model of the observed pH-dependence of the binding constants, defined by Chasteen and Williams.[26]

Parameter	Tf+S	Tf−S
$f_{sp,\,min}$	0.58	0.55
$f_{sp,\,max}$	34.8	36.9
pK'_a	6.47	6.25
n'	4.73	6.45
R^2	>0.999	>0.999

[a] If a significant single-point outlier is omitted from the titration of Tf−S, the following adjusted values result: pK'_a = 6.24, n' = 6.32.

10. Conflicts of interest

There are no conflicts of interest to declare.

11. Acknowledgements

This work was supported by funding from the Croatian Science Foundation grant UIP-2017-05-9537 – Glycosylation as a factor in the iron transport mechanism of human serum transferrin (GlyMech). Valentina Borko was additionally financed by the Croatian Science Foundation grant DOK-2018-09-1042. Additional support was provided by the European Regional Development Fund grants for 'Strengthening of Scientific Research and Innovation Capacities of the Faculty of Pharmacy and Biochemistry at the University of Zagreb' (KK.01.1.1.02.0021), 'Development of methods for production and labelling of glycan standards for molecular diagnostics' (KK.01.1.1.07.0055) and 'Scientific center of excellence for personalized health care' (KK.01.1.1.01.0010).

12. Notes and references

1 V. Borko, T. Friganović and T. Weitner, *Anal. Methods*, 2023, **15**, 6499–6513.
2 T. Friganović, A. Tomašić, T. Šeba, I. Biruš, R. Kerep, V. Borko, D. Šakić, M. Gabričević and T. Weitner, *Heliyon*, 2021, **7**, e08030.
3 T. Friganović, V. Borko and T. Weitner, *Maced. Pharm. Bull.*, 2022, **68**, 415–416.
4 T. Weitner, T. Friganović and D. Šakić, *Anal. Chem.*, 2022, **94**, 7107–7114.
5 J. R. Lakowicz, Ed., in *Principles of Fluorescence Spectroscopy*, Springer US, Boston, MA, 2006, pp. 27–61.
6 T. Friganović and T. Weitner, *Anal. Chem.*, 2023, **95**, 13036–13045.
7 S. Kumar Panigrahi and A. Kumar Mishra, *Journal of Photochemistry and Photobiology C: Photochemistry Reviews*, 2019, **41**, 100318.
8 I. Jarmoskaite, I. AlSadhan, P. P. Vaidyanathan and D. Herschlag, *eLife*, 2020, **9**, e57264.
9 D. Jenkins, Solving Quadratic, Cubic, Quartic and higher order equations; examples, https://newtonexcelbach.com/2014/01/14/solving-quadratic-cubic-quartic-and-higher-order-equations-examples/, (accessed April 27, 2024).
10 M. A. Jenkins and J. F. Traub, *Commun. ACM*, 1972, **15**, 97–99.
11 H. D. B. Jenkins and K. P. Thakur, *J. Chem. Educ.*, 1979, **56**, 576.
12 A. Ralston and P. Rabinowitz, *A first Course in numerical analysis*, McGraw-Hill, Auckland, 2. ed., 1984.
13 A. Ringbom and E. Still, *Analytica Chimica Acta*, 1972, **59**, 143–146.
14 R. J. Motekaitis and A. E. Martell, *Journal of Coordination Chemistry*, 1994, **31**, 67–78.
15 J. Hegenauer, P. Saltman and G. Nace, *Biochemistry*, 1979, **18**, 3865–3879.
16 W. R. Harris and V. L. Pecoraro, *Biochemistry*, 1983, **22**, 292–299.
17 R. L. Anderson, W. E. Bishop, R. L. Campbell and G. C. Becking, *CRC Critical Reviews in Toxicology*, 1985, **15**, 1–102.
18 R. M. Smith and A. E. Martell, *Critical Stability Constants*, Springer US, Boston, MA, 1989.
19 T. Knepper, *TrAC Trends in Analytical Chemistry*, 2003, **22**, 708–724.
20 E. Repo, J. K. Warchoł, A. Bhatnagar, A. Mudhoo and M. Sillanpää, *Water Research*, 2013, **47**, 4812–4832.
21 D. C. Harris, *J. Chem. Educ.*, 1998, **75**, 119.
22 J. C. Dechaux, V. Zimmermann and V. Nollet, *Atmospheric Environment*, 1994, **28**, 195–211.
23 V. Borko, T. Friganović and T. Weitner, *Journal of Inorganic Biochemistry*, 2023, **244**, 112207.
24 P. Armitage, G. Berry and J. N. S. Matthews, *Statistical Methods in Medical Research*, Wiley, 1st edn., 2002.
25 T. Weitner, T. Friganovic and V. Borko, Protein sialylation affects the pH-dependent binding of ferric ion to human serum transferrin - experimental data, Zenodo, 2024, https://doi.org/10.5281/zenodo.10881688.
26 N. D. Chasteen and J. Williams, *Biochemical Journal*, 1981, **193**, 717–727.